12-2009

# Copper(I) Complexes of Heterocyclic Thiourea Ligands

Aakarsh Saxena

Emily C. Dugan

Jeffrey Liaw

Matthew D. Dembo

Robert D. Pike
*William & Mary*, rdpike@wm.edu



## Recommended Citation

Saxena, Aakarsh; Dugan, Emily C.; Liaw, Jeffrey; Dembo, Matthew D.; and Pike, Robert D., Copper(I) Complexes of Heterocyclic Thiourea Ligands (2009). *Polyhedron*, 28(18), 4017-4031. https://doi.org/10.1016/j.poly.2009.08.023

# Copper(I) Complexes of Heterocyclic Thiourea Ligands.

Aakarsh Saxena, Emily C. Dugan, Jeffrey Liaw, Matthew D. Dembo and Robert D. Pike*

*Department of Chemistry, College of William and Mary, Williamsburg, VA 23187.*

Abstract: The coordination of heterocyclic thiourea ligands (L = *N*-(2-pyridyl)-*N´*-phenylthiourea (**1**), *N*-(2-pyridyl)-*N´*-methylthiourea (**2**), *N*-(3-pyridyl)-*N´*-phenylthiourea (**3**), *N*-(3-pyridyl)-*N´*-methylthiourea (**4**), *N*-(4-pyridyl)-*N´*-phenylthiourea (**5**), *N*-(2-pyrimidyl)-*N´*-phenylthiourea (**6**), *N*-(2-pyrimidyl)-*N´*-methylthiourea (**7**), *N*-(2-thiazolyl)-*N´*-methylthiourea (**8**), *N*-(2-benzothiazolyl)-*N´*-methylthiourea (**9**), *N*,*N´*-bis(2-pyridyl)thiourea (**10**) and *N*,*N´*-bis(3-pyridyl)thiourea (**11**) with CuX (X = Cl, Br, I, $NO_3$) has been investigated. CuX:L product stoichiometries of 1:1 – 1:5 were found, with 1:1 being most common. X-ray structures of four 3-coordinate mononuclear $CuXL_2$ complexes ($CuCl(\mathbf{6})_2$, $CuCl(\mathbf{7})_2$, $CuBr(\mathbf{6})_2$, and $CuBr(\mathbf{9})_2$) are reported. In contrast, $CuBr(\mathbf{1})_2$ is a 1D sulfur-bridged polymer. CuIL structures (L = **7**, **8**) are 1D chains with corner-sharing $Cu_2(\mu\text{-}I)_2$ and $Cu_2(\mu\text{-}S)_2$ units, and CuCl(**10**) is a 2D network having μ-Cl and N-/S-bridging L. Two $[CuL_2]NO_3$ structures are reported: a mononuclear 4-coordinate copper complex with chelating ligands (L = **10**) and a 1D link-chain with N-/S-bridging L (L = **3**). Two ligand oxidative cyclizations were encountered during crystallization. CuI crystallized with **6** to produce zigzag ladder polymer $[(CuI)_2(\mathbf{12})]\bullet 2CH_3CN$ (**12** = N-(pyrimidin-2-yl)benzo[d]thiazol-2-amine) and $CuNO_3$ crystallized with **10** to form $[Cu_2(NO_3)(\mathbf{13})_2(MeCN)]NO_3$ (**13** = dipyridyltetraazathiapentalene).

Keywords: Copper complexes; Crystal structures; Thiourea ligands; Heterocycles; Metal-organic networks; Oxidative cyclization

## 1. Introduction

The self-assembly of transition metals with bridging ligands to produce metal-organic networks (MONs) is currently a very active area of study [1]. Copper(I) centers are especially flexible with respect to coordination environment [2], ranging from 2- to 4-coordinate (see examples in Chart 1 below). However, also important in MON formation are the bonding capabilities of the ligands chosen. A recent review has divided MONs according to dimensionality produced through organic vs. inorganic ligand bridging [3]. According to the authors' scheme, the 2D network CuBr(Pyz) (Pyz = pyrazine) [4] would be classified as $I^1O^1$, since the inorganic ligand bromide links the copper atoms into 1D chains ($I^1$) and the organic Pyz ligand links them in a perpendicular direction ($O^1$). The sum of the exponents gives the overall dimensionality of the MON, a 2D sheet in this case.

Halide bridging behavior in MONs such as CuBr(Pyz) may be described as single-atom-bridging (SAB). Unlike conventional organic bridging ligands, such as Pyz or 4,4′-bipyridine, which have two or more widely separated and geometrically constrained lone pair-bearing atoms, SAB ligands have two or more lone pairs residing on a single atom and consequently form short bridges between two or more metal centers. While group 16 or 17 anions are obvious candidates for SAB behavior, organic SAB examples are also known. One important group of organic SABs is comprised of thiocarbonyl compounds. A remarkable collection of copper(I) networks with thiourea ligands is known, many showing sulfur SAB behavior [5]. The Cu(I) centers bridged by thiocarbonyl sulfur (S) and halide SABs (X) can form rhomboid $Cu_2X_2$ or $Cu_2S_2$ dimers, $Cu_4X_4$ or $Cu_4S_4$ cubane tetramers, $(Cu_2X_2)_n$ or $(Cu_2S_2)_n$ stair step polymers, and $(CuX)_n$ or $(CuS)_n$ chains [2]. Examples of SAB complexes are shown in Chart 1. As is suggested by the variety of the products shown in Chart 1, it can be very difficult to predict aforehand when sulfur or halide

atoms will act in SAB fashion and when they will remain monodentate. In addition, halide ions can also act as outer sphere anions.

Chart 1

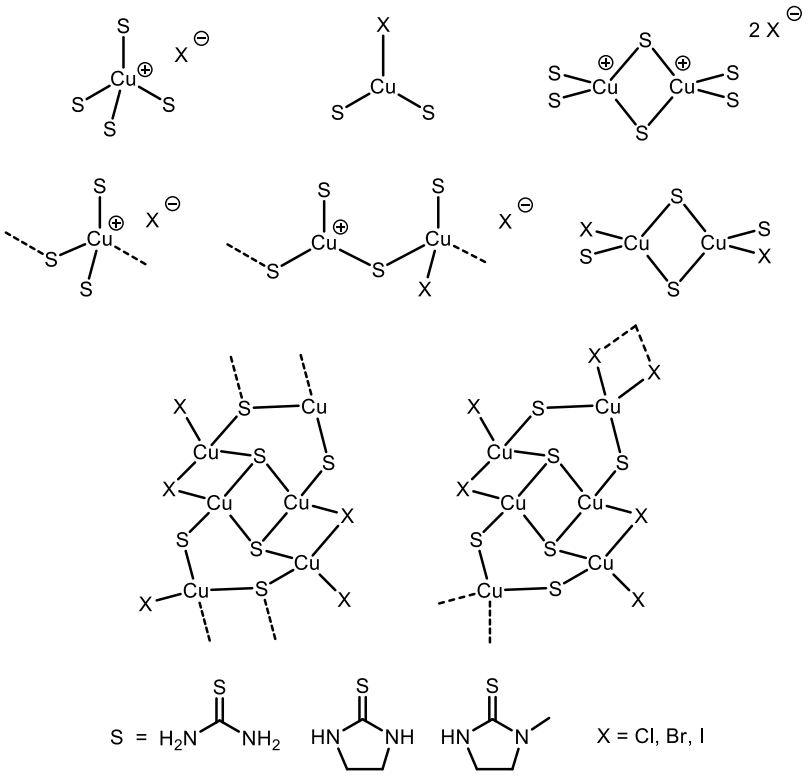


In the following study we have examined the network-forming behavior of thiourea ligands bearing nitrogen heterocycle groups with copper(I) halides and nitrate. The heterocyclic thiourea molecules (HetTu) **1**–**11** shown in Chart 2 are themselves network-formers through hydrogen-bonding [6]. It was expected that they would show a variety of bridging behaviors involving the sulfur (monodentate or SAB) and nitrogen centers, leading to network formation. Additional network-forming behavior was anticipated from the halide (SAB) and possibly the nitrate ions. To date, a single HetTu complex of copper(I) has been reported [7]. This compound is $[Cu(\mathbf{10})_2]ClO_4$. It is monomeric, with a single 4-coordinate copper coordinated to sulfur and one pyridyl nitrogen from each ligand. The remaining pyridyl nitrogen on each ligand engages in intramolecular hydrogen-bonding with a thiourea N–H. The Zn(II) complex is similar. However,

more complicated and highly networked structures are to be expected when the pyridyl groups and thiocarbonyl sulfur are geometrically prevented from chelating a single metal center.

Chart 2

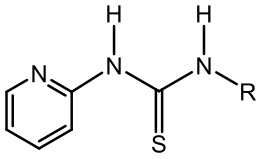

R = Ph,**1**; R = Me, **2**

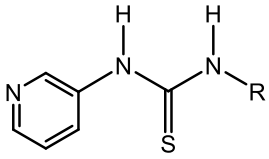

R = Ph, **3**; R = Me, **4**

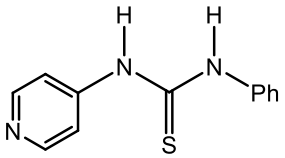

**5**

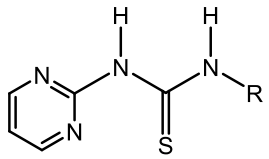

R = Ph, **6**; Me, **7**

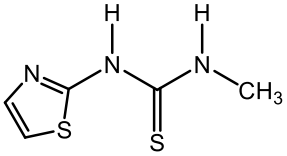

**8**

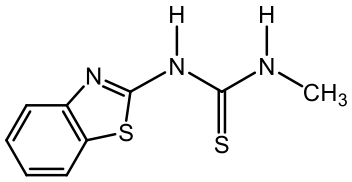

**9**

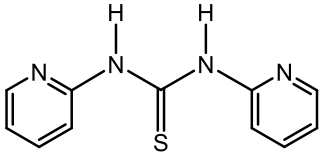

**10**

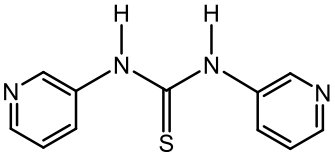

**11**

## 2. Experimental

### *2.1. General methods*

All syntheses were carried out under nitrogen atmosphere. Microanalyses for C, H, and N were carried out by Atlantic Microlab, Inc., Norcross, GA. HetTu ligands, *N*-(2-pyridyl)-*N´*-phenylthiourea (**1**), *N*-(2-pyridyl)-*N´*-methylthiourea (**2**), *N*-(3-pyridyl)-*N´*-phenylthiourea (**3**), *N*-(3-pyridyl)-*N´*-methylthiourea (**4**), *N*-(4-pyridyl)-*N´*-phenylthiourea (**5**), *N*-(2-pyrimidyl)-*N´*-

phenylthiourea (**6**), *N*-(2-pyrimidyl)-*N´*-methylthiourea (**7**), *N*-(2-thiazolyl)-*N´*-methylthiourea (**8**), *N*-(2-benzothiazolyl)-*N´*-methylthiourea (**9**), *N*,*N´*-bis(2-pyridyl)thiourea (**10**) and *N*,*N´*-bis(3-pyridyl)thiourea (**11**), were synthesized as previously described [6]. Copper(I) chloride and bromide were freshly recrystallized from aqueous HCl or HBr. Copper(I) iodide was used as received from Aldrich. Copper(I) nitrate was prepared *in situ* by conproportionation of $Cu(NO_3)_2$•$2.5H_2O$ in MeCN as described below.

*2.2. Syntheses*

*2.2.1. Synthesis of CuCl(**1**)$_2$*

Copper(I) chloride (99 mg, 1.00 mmol) was dissolved in 25 mL MeCN under $N_2$. **1** (229 mg, 1.00 mmol) was added as a solid. The resulting suspension was stirred under nitrogen for 1 h at room temp. The white solid was collected via filtration, and washed with diethyl ether. It was dried under vacuum (184 mg, 68.5% yield). Anal. Calcd for $C_{24}H_{22}N_6ClCuS_2$: C, 51.70; H, 3.98; N, 15.70. Found: C, 52.08; H, 3.97; N, 15.13.

*2.2.2. Synthesis of [CuBr(**1**)]•MeCN*

The procedure for *CuCl(**1**)$_2$* was followed using CuBr. A grey-green solid was isolated (77.6%). Anal. Calcd for $C_{14}H_{14}N_4BrCuS$: C, 40.64; H, 3.41; N, 13.54. Found: C, 42.44; H, 3.42; N, 13.53.

*2.2.3. Synthesis of CuI(**1**)*

The procedure for *CuCl(**1**)$_2$* was followed using CuI. An off-white solid was isolated (94.5%). Anal. Calcd for $C_{12}H_{11}N_3CuIS$: C, 34.34; H, 2.64; N, 10.01. Found: C, 34.24; H, 2.63; N, 10.05.

*2.2.4. Synthesis of CuNO$_3$(**1**)*

$Cu(NO_3)_2$•$2.5H_2O$ (116 mg, 0.500 mmol) and excess copper wool were stirred under $N_2$ in 25 mL MeCN for 30 min. until the blue solution color was discharged. The copper wool was removed and **1** (229 mg, 1.00 mmol) was added as a solid. The resulting suspension was stirred

under nitrogen for 1 h at room temp. This resulted in a precipitate. The solid was collected via filtration, and was washed with diethyl ether. The light brown solid was dried under vacuum (226 mg, 63.8% yield). Anal. Calcd for $C_{12}H_{11}N_4CuO_3S$: C, 40.62; H, 3.12; N, 15.79. Found: C, 42.23; H, 3.06; N, 15.85.

*2.2.5. Synthesis of $(CuCl)_2$(**2**)$_3$*

The procedure for *CuCl(**1**)$_2$* was followed using CuCl and **2**. A white solid was isolated (75.1%). Anal. Calcd for $C_{21}H_{27}N_9Cl_2Cu_2S_3$: C, 36.05; H, 3.89; N, 18.02. Found: C, 35.88; H, 3.81; N, 17.81.

*2.2.6. Synthesis of [CuBr(**2**)]•MeCN*

The procedure for *CuCl(**1**)$_2$* was followed using CuBr and **2**. A white solid was isolated (59.1%). Anal. Calcd for $C_9H_{12}N_4CuBrS$: C, 30.73; H, 3.44; N, 15.93. Found: C, 31.41; H, 3.43; N, 15.62.

*2.2.7. Synthesis of [CuI(**2**)]•MeCN*

The procedure for compound **1a** was followed using CuI and **2**. A cream solid was isolated (88.2%). Anal. Calcd for $C_9H_{12}N_4CuIS$: C, 27.11; H, 3.03; N, 14.05. Found: C, 27.88; H, 3.01; N, 13.86.

*2.2.8. Synthesis of [CuNO$_3$(**2**)]•MeCN*

The procedure for *CuNO$_3$(**1**)* was followed using **2**. A pale yellow solid was isolated (89.2%). Anal. Calcd for $C_9H_{12}N_5CuO_3S$: C, 32.38; H, 3.62; N, 20.98. Found: C, 31.97; H, 3.51; N, 20.65.

*2.2.9. Synthesis of CuCl(**3**)$_4$*

The procedure for *CuCl(**1**)$_2$* was followed using CuCl and **3**. A yellow solid was isolated (83.8%). Anal. Calcd for $C_{48}H_{44}N_{12}ClCuS_4$: C, 56.73; H, 4.36; N, 16.54. Found: C, 56.08; H, 4.40; N, 16.33.

*2.2.10. Synthesis of CuBr(**3**)$_2$*

The procedure for *CuCl(**1**)$_2$* was followed using CuBr and **3**. A straw-colored solid was isolated (87.7%). Anal. Calcd for $C_{24}H_{22}N_6BrCuS_2$: C, 47.88; H, 3.68; N, 13.96. Found: C, 48.79; H, 3.78; N, 14.09.

*2.2.11. Synthesis of CuI(**3**)*

The procedure for *CuCl(**1**)$_2$* was followed using CuI and **3**. A pale yellow solid was isolated (86.2%). Anal. Calcd for $C_{12}H_{11}N_3CuIS$: C, 34.34; H, 2.64; N, 10.01. Found: C, 33.62; H, 2.66; N, 10.22.

*2.2.12. Synthesis of [CuNO$_3$(**3**)]•MeCN*

The procedure for *CuNO$_3$(**1**)* was followed using **3**. A yellow solid was isolated (90.4%). Anal. Calcd for $C_{14}H_{14}N_5CuO_3S$: C, 42.47; H, 3.56; N, 17.69. Found: C, 42.48; H, 3.64; N, 17.43.

*2.2.13. Synthesis of CuCl(**4**)*

The procedure for *CuCl(**1**)$_2$* was followed using CuCl and **4**. A yellow solid was isolated (69.5%). Anal. Calcd for $C_7H_9N_3ClCuS$: C, 31.58; H, 3.41; N, 15.78. Found: C, 32.20; H, 3.46; N, 15.95.

*2.2.14. Synthesis of CuBr(**4**)*

The procedure for *CuCl(**1**)$_2$* was followed using CuBr and **4**. A cream solid was isolated (62.9%). Anal. Calcd for $C_7H_9N_3BrCuS$: C, 27.06; H, 2.92; N, 13.53. Found: C, 26.46; H, 2.83; N, 13.12.

*2.2.15. Synthesis of CuI(**4**)*

The procedure for *CuCl(**1**)$_2$* was followed using CuI and **4**. A white solid was isolated (94.1%). Anal. Calcd for $C_7H_9N_3CuIS$: C, 23.51; H, 2.54; N, 11.75. Found: C, 23.57; H, 2.57; N, 11.56.

*2.2.16. Synthesis of (CuNO$_3$)$_2$(**4**)$_3$*

The procedure for *CuNO$_3$(**1**)* was followed using **4**. A cream solid was isolated (86.5%). Anal. Calcd for $C_{21}H_{27}N_{11}Cu_2O_6S_3$: C, 33.51; H, 3.62; N, 20.47. Found: C, 32.78; H, 3.80; N, 20.30.

*2.2.17. Synthesis of CuCl(**5**)*

The procedure for *CuCl(**1**)*$_2$ was followed using CuCl and **5**. A yellow solid was isolated (74.0%). Anal. Calcd for $C_{12}H_{11}N_3ClCuS$: C, 43.90; H, 3.38; N, 12.80. Found: C, 43.69; H, 3.32; N, 12.88.

*2.2.18. Synthesis of CuBr(**5**)*

The procedure for *CuCl(**1**)*$_2$ was followed using CuBr and **5**. A yellow solid was isolated (48.4%). Anal. Calcd for $C_{12}H_{11}N_3BrCuS$: C, 38.67; H, 2.97; N, 11.27. Found: C, 39.07; H, 3.04; N, 11.62.

*2.2.19. Synthesis of CuI(**5**)*

The procedure for *CuCl(**1**)*$_2$ was followed using CuI and **5**. A yellow solid was isolated (82.3%). Anal. Calcd for $C_{12}H_{11}N_3CuIS$: C, 34.34; H, 2.64; N, 10.01. Found: C, 34.89; H, 2.66 N, 9.91.

*2.2.20. Synthesis of (CuNO$_3$)$_2$(**5**)$_3$*

The procedure for *CuNO$_3$(**1**)* was followed using **5**. A yellow solid was isolated (57.8%). Anal. Calcd for $C_{36}H_{33}N_{11}Cu_2O_6S_3$: C, 46.05; H, 3.54; N, 16.41. Found: C, 45.02; H, 3.48; N, 15.64.

*2.2.21. Synthesis of CuCl(**6**)*$_2$

The procedure for *CuCl(**1**)*$_2$ was followed using CuCl and **6**. A white solid was isolated (85.1%). Anal. Calcd for $C_{22}H_{20}N_8ClCuS_2$: C, 47.22; H, 3.60; N, 20.02. Found: C, 47.19; H, 3.66; N, 19.76.

*2.2.22. Synthesis of CuBr(**6**)*$_2$

The procedure for *CuCl(**1**)*$_2$ was followed using CuBr and **6**. A white solid was isolated (70.2%). Anal. Calcd for $C_{22}H_{20}N_8BrCuS_2$: C, 43.75; H, 3.34; N, 18.55. Found: C, 43.47; H, 3.21; N, 18.27.

*2.2.23. Synthesis of CuI(**6**)*

The procedure for *CuCl(**1**)$_2$* was followed using CuI and **6**. A yellow solid was isolated (54.2%). Anal. Calcd for $C_{11}H_{10}N_4CuIS$: C, 31.40; H, 2.40; N, 13.32. Found: C, 30.67; H, 2.35; N, 13.07.

*2.2.24. Synthesis of CuNO$_3$(**6**)$_2$*

The procedure for *CuNO$_3$(**1**)* was followed using **6**. A yellow solid was isolated (79.8%). Anal. Calcd for $C_{22}H_{20}N_9CuO_3S_2$: C, 45.08; H, 3.44; N, 21.51. Found: C, 45.14; H, 3.44; N, 21.51.

*2.2.25. Synthesis of CuCl(**7**)$_4$*

The procedure for *CuCl(**1**)$_2$* was followed using CuCl and **7**. A white solid was isolated (85.0%). Anal. Calcd for $C_{24}H_{32}N_{16}ClCuS_4$: C, 37.35; H, 4.18; N, 29.03. Found: C, 37.84; H, 4.27; N, 29.22.

*2.2.26. Synthesis of CuBr(**7**)*

The procedure for *CuCl(**1**)$_2$* was followed using CuBr and **7**. A pale yellow solid was isolated (78.5%). Anal. Calcd for $C_6H_8N_4BrCuS$: C, 23.12; H, 2.59; N, 17.98. Found: C, 23.47; H, 2.59; N, 17.99.

*2.2.27. Synthesis of CuI(**7**)*

The procedure for *CuCl(**1**)$_2$* was followed using CuI and **7**. A pale yellow solid was isolated (97.5%). Anal. Calcd for $C_6H_8N_4CuIS$: C, 20.09; H, 2.25; N, 15.62. Found: C, 20.33; H, 2.29; N, 15.66.

*2.2.28. Synthesis of CuNO$_3$(**7**)$_2$*

The procedure for *CuNO$_3$(**1**)* was followed using **7**. A yellow solid was isolated (71.4%). Anal. Calcd for $C_{18}H_{24}N_{14}Cu_2O_6S_3$: C, 28.61; H, 3.20; N, 25.95. Found: C, 29.07; H, 3.19; N, 25.46.

*2.2.29. Synthesis of (CuCl)$_2$(**8**)$_3$*

The procedure for *CuCl(**1**)$_2$* was followed using CuCl and **8**. A white solid was isolated (57.3%). Anal. Calcd for $C_{15}H_{21}N_9Cl_2Cu_2S_6$: C, 25.10; H, 2.95; N, 17.56. Found: C, 25.24; H, 2.93; N, 17.50.

*2.2.30. Synthesis of (CuBr)$_2$(**8**)$_3$*

The procedure for *CuCl(**1**)$_2$* was followed using CuBr and **8**. A cream solid was isolated (80.5%). Anal. Calcd for $C_{15}H_{21}N_9Br_2Cu_2S_6$: C, 22.33; H, 2.62; N, 15.63. Found: C, 22.53; H, 2.63; N, 15.66.

*2.2.31. Synthesis of CuI(**8**)*

The procedure for *CuCl(**1**)$_2$* was followed using CuI and **8**. A yellow solid was isolated (68.6%). Anal. Calcd for $C_5H_7N_3CuIS_2$: C, 16.51; H, 1.94; N, 11.55. Found: C, 16.90; H, 1.93; N, 11.58.

*2.2.32. Synthesis of CuNO$_3$(**8**)$_2$*

The procedure for *CuNO$_3$(**1**)* was followed using **8**. A light brown solid was isolated (12.7%). Anal. Calcd for $C_{10}H_{14}N_7CuO_3S_4$: C, 25.44; H, 2.99; N, 20.77. Found: C, 25.41; H, 2.80; N, 20.16.

*2.2.33. Synthesis of [CuCl(**9**)]•2MeCN*

The procedure for *CuCl(**1**)$_2$* was followed using CuCl and **9**. A pale yellow solid was isolated (87.6%). Anal. Calcd for $C_{10}H_{10.5}N_{3.5}ClCuS_2$: C, 35.03; H, 3.09; N, 14.30. Found: C, 35.20; H, 3.03; N, 13.85.

*2.2.34. Synthesis of CuBr(**9**)*

The procedure for *CuCl(**1**)$_2$* was followed using CuBr and **9**. An off-white solid was isolated (72.0%). Anal. Calcd for $C_9H_9N_3BrCuS_2$: C, 29.47; H, 2.47; N, 11.46. Found: C, 29.17; H, 2.57; N, 11.31.

*2.2.35. Synthesis of (CuI)$_2$(**9**)$_3$*

The procedure for *CuCl(**1**)$_2$* was followed using CuI and **9**. A cream solid was isolated (88.8%). Anal. Calcd for $C_{27}H_{27}N_9Cu_2I_2S_6$: C, 30.86; H, 2.59; N, 12.00. Found: C, 30.04; H, 2.58; N, 11.88.

*2.2.36. Synthesis of [CuNO$_3$(**9**)]•MeCN*

The procedure for *CuNO$_3$(**1**)* was followed using **9**. A light yellow solid was isolated (63.4%). Anal. Calcd for $C_{11}H_{12}N_5CuO_3S_2$: C, 33.88; H, 3.10; N, 17.96. Found: C, 34.32; H, 3.07; N, 17.38.

*2.2.37. Synthesis of (CuCl)$_2$(**10**)$_3$*

The procedure for *CuCl(**1**)$_2$* was followed using CuCl and **10**. A yellow solid was isolated (68.7%). Anal. Calcd for $C_{33}H_{30}N_{12}Cl_2Cu_2S_3$: C, 44.59; H, 3.40; N, 18.91. Found: C, 43.54; H, 3.36; N, 18.63.

*2.2.38. Synthesis of CuBr(**10**)*

The procedure for *CuCl(**1**)$_2$* was followed using CuBr and **10**. A yellow solid was isolated (79.7%). Anal. Calcd for $C_{11}H_{10}N_4BrCuS$: C, 35.35; H, 2.70; N, 14.99. Found: C, 35.11; H, 2.74; N, 15.08.

*2.2.39. Synthesis of CuI(**10**)*

The procedure for *CuCl(**1**)$_2$* was followed using CuI and **10**. A cream solid was isolated (79.0%). Anal. Calcd for $C_{11}H_{10}N_4CuIS$: C, 31.40; H, 2.40; N, 13.32. Found: C, 31.50; H, 2.46; N, 13.47.

*2.2.40. Synthesis of [(CuNO$_3$)$_2$(**10**)$_3$]•MeCN*

The procedure for *CuNO$_3$(**1**)* was followed using **10**. A yellow solid was isolated (24.8%). Anal. Calcd for $C_{35}H_{33}N_{15}Cu_2O_6S_3$: C, 42.76; H, 3.38; N, 21.37. Found: C, 43.11; H, 3.44; N, 20.91.

*2.2.41. Synthesis of CuNO$_3$(**10**)$_2$*

The procedure for *$CuNO_3$(**1**)* was followed using **10** and stirring for 4 h. An orange solid was isolated (45.0%). Anal. Calcd for $C_{22}H_{20}N_9CuO_3S_2$: C, 45.08; H, 3.44; N, 21.51. Found: C, 45.05; H, 3.41; N, 21.50.

*2.2.42. Synthesis of CuCl(**11**)$_4$*

The procedure for *CuCl(**1**)$_2$* was followed using CuCl and **11**. A pale green solid was isolated (81.9%). Anal. Calcd for $C_{44}H_{40}N_{16}ClCuS_4$: C, 51.80; H, 3.95; N, 21.97. Found: C, 52.09; H, 3.97; N, 21.79.

*2.2.43. Synthesis of CuBr(**11**)$_5$*

The procedure for *CuCl(**1**)$_2$* was followed using CuBr and **11**. An off-white solid was isolated (90.7%). Anal. Calcd for $C_{55}H_{50}N_{20}BrCuS_5$: C, 51.02; H, 3.89; N, 21.63. Found: C, 51.71; H, 3.98; N, 21.62.

*2.2.44. Synthesis of CuI(**11**)$_4$*

The procedure for *CuCl(**1**)$_2$* was followed using CuI and **11**. A cream solid was isolated (82.9%). Anal. Calcd for $C_{44}H_{40}N_{16}CuIS_4$: C, 47.54; H, 3.63; N, 20.16. Found: C, 48.44; H, 3.78; N, 20.48.

*2.2.45. Synthesis of [$CuNO_3$(**11**)]•MeCN*

The procedure for *$CuNO_3$(**1**)* was followed using **11**. A yellow solid was isolated (80.4%). Anal. Calcd for $C_{13}H_{13}N_6CuO_3S$: C, 39.34; H, 3.30; N, 21.17. Found: C, 39.77; H, 3.36; N, 20.94.

*2.3. X-ray data collection, structure solutions and refinements*

Crystals were grown in 5 mm tubes by two techniques. Solution concentrations were 20 mM. Typically, CuX was dissolved in MeCN and layered with a HetTu dissolved in MeCN. When the HetTu was insoluble in MeCN, the HetTu was dissolved in acetone. In successful cases, X-ray quality crystals formed in about a week. All measurements were made using graphite-monochromated Cu Kα radiation on a Bruker-AXS three-circle diffractometer, equipped

with a SMART Apex II CCD detector. Initial space group determination was based on a matrix consisting of 120 frames. The data were corrected for Lorentz and polarization [8] effects and absorption using SADABS [9]. The structures were solved by use of direct methods or Patterson map. Least squares refinement on $F^2$ was used for all reflections. Structure solution, refinement and the calculation of derived results were performed using the SHELXTL [10] package of software. The non-hydrogen atoms were refined anisotropically. For CuCl(**10**), CuCl(**6**), and $CuNO_3$(**10**) all hydrogens were refined. For CuBr(**6**) and CuCl(**7**) some hydrogens were refined. In all other cases, all hydrogen atoms were located then placed in theoretical positions. Acetone molecules (1.5/copper) were present in the structure of $[Cu(\mathbf{3})_2]NO_3$. These very badly disordered solvent molecules were eliminated from the structure using Platon SQUEEZE [11]. The half-independent MeCN molecule in $[(CuI)_2(\mathbf{12})]\bullet 2CH_3CN$ was badly disordered and was only partially modeled. For CuI(**9**), fairly large (>2 e/Å$^3$) residual peaks remained near the iodine atom after refinement. This was clearly the result of imperfect absorption correction, despite the use of a face-indexed model. Crystallographic parameters for all complexes are provided in Table 2. Selected bond lengths and angles are provided in Table 3.

## 3. Results and Discussion

### *3.1. Synthesis and Stoichiometry of Bulk Products*

The reactions of copper(I) salts, CuX (X = Cl, Br, I, $NO_3$), with various HetTu were carried out using a 1:1 metal salt:HetTu ratio. Copper(I) nitrate was prepared in MeCN through conproportionation of $Cu(NO_3)_2\bullet 2.5H_2O$ and Cu and was used without isolation. The HetTu ligands were added to MeCN solutions of CuX, either as solutions or suspensions in MeCN. In all cases solid products were obtained after stirring for an hour at room temperature. The various stoichiometric trends are summarized in Table 1. As is evident in Table 1, a remarkable variety of CuX:HetTu product ratios was found. The stoichiometries noted in the bulk synthesis products spanned a wide range from the Cu-rich 1:1 to the very HetTu-rich 1:5. Some general comments

about metal-to-ligand ratio in these complexes are in order. It should be expected that metal-rich product ratios are indicative of ligand bridging behavior, since when there are fewer ligands each must occupy more metal coordination sites. Copper(I) shows a roughly equal preference for 3- and 4-coordination. So CuX:HetTu ratios of less than 1:2 are highly suggestive of network formation.

The 1:1 CuX:HetTu ratio was the most common among the bulk synthesis products, occurring (with or without MeCN present in the product) in 25 of 45 cases. As rationalized above, a copper-rich ratio of 1:1 suggests some sort of ligand bridging behavior. As is evident from Chart 1 and the X-ray crystal structures discussed below, there are a variety of ways in which bridging can occur with the ligands used in this study. The halides and HetTu sulfur atom can engage in SAB behavior and the HetTu and nitrate can bridge through pairs of heteroatoms. Of course in the eight 1:1 complexes that also have MeCN present, the solvent may act as a ligand, obviating network formation. The solvent-free 1:1 cases in which ligand bridging need not occur would be the complexes of HetTu having ortho-type heteroatoms (**1**,**2**,**6**–**10**), since these ligands can potentially chelate through a combination of S- and heterocycle N-coordination [7]. The prevalence of 1:1 stoichiometry found in this study favors CuI and CuBr products over those of CuCl and $CuNO_3$. This fact is not surprising given the greater tendency of larger halides to engage in SAB behavior. Like 1:1 stoichiometry, the 2:3 ratio seen in nine additional bulk products is probably also indicative of ligand-bridging.

The moderately ligand-rich 1:2 stoichiometry was found in six instances. This ratio is most likely reflective of monomeric species $CuX(HetTu)_2$ (although dimer or polymer formation is also possible, see the structure of $CuBr(\mathbf{1})_2$ below). No 1:3 species, $CuX(HetTu)_3$, were encountered. Four 1:4 CuX:HetTu complexes were found, presumably representing $[Cu(HetTu)_4]X$. The single 1:5 species uncovered herein, $CuBr(\mathbf{11})_5$ is quite remarkable. Since copper(I) has virtually no tendency to form 5-coordinate complexes, one can only speculate that

the extra ligand(s) are trapped in the lattice of CuBr(**11**)$_n$ ($n$ = 3 or 4), possibly through hydrogen-bonding interactions.

Reaction time was varied for a number of combinations studied herein. However, in only one case were two separate bulk products encountered. Combination of $CuNO_3$ with **10** resulted in the immediate formation of a yellow precipitate which, when isolated, revealed a yellow product, [$(CuNO_3)_2$(**10**)$_3$]•MeCN, based on analytical data. When the reaction time scale was lengthened to four hours, the initial yellow precipitate gave way to an orange solid. Elemental analysis results confirmed that the latter complex was $CuNO_3$(**10**)$_2$.

*3.1. Description of X-Ray Structures*

A total of twelve crystal structures were solved during the course of this study. Surprisingly, two of these revealed cyclization of the thioureas to form thiazoles (see below). In both cases ligand oxidation resulted in the loss of $H_2$. Although no analytical evidence of such a transformation was noted in the bulk synthesis products described above, the analytical difference due to $H_2$ loss would be fairly small. Also remarkable was the fact that of the remaining ten structures, only four showed stoichiometry in agreement with that of the corresponding bulk synthesis product (see Table 1).

*3.1.1. Monomeric Complexes ($I^0O^0$)*

Two types of monomeric compounds were encountered in the current study. The first type that we will consider are halide complexes having 1:2 CuX:HetTu ratio and 3-coordinate copper. Four such complexes were identified: CuCl(**6**)$_2$, CuCl(**7**)$_2$, CuBr(**6**)$_2$, and CuBr(**9**)$_2$. The two complexes of **6** showed the identical 1:2 stoichiometry in the bulk, while the other complexes did not. In all four cases, two crystallographically independent HetTu ligands and a terminal halide ligand were bound to a single copper center. Structural diagrams for CuCl(**6**)$_2$ and CuBr(**9**)$_2$ are provided in Figures 1A and 1B. The four 3-coordinate monomeric structures are

overlaid in Figure 1C, roughly aligning an S–Cu–X sequence of atoms. As is evident, the structures are highly analogous, showing trigonal planar copper angles very close to 120°. In each of these compounds, and in fact all but one of the structures presented herein, the thioureas adopt E,Z conformations [6]. This arrangement results from an intra-ligand hydrogen-bond between a thiourea N–H and a heterocycle nitrogen (e.g. N2–H···N6 and N4–H···N7 in Figure 1A, see Table S1 for a complete list of H-bonds). In all four structures, weak hydrogen-bonding type interactions exist between the halogen and two thiourea nitrogen atoms (e.g. N1–H···Cl1 and N3–H···Cl1 in Figure 1A). No intermolecular hydrogen-bonding is evident in these structures. In all four compounds, three nearly coplanar central atom planes may be identified: two NC(S)N and SCu(X)S (see Table S2), although in CuBr(**1**) the copper atom shows a significant –0.4106(3) Å displacement from the best SCu(X)S plane. The heterocycle rings that are oriented toward the halogen atom in each compound are nearly coplanar with these central planes. When a second HetTu ring is present, it is oriented away from the halogen and is not coplanar with the central plane (see Figures 1A and 1C and Table S2).

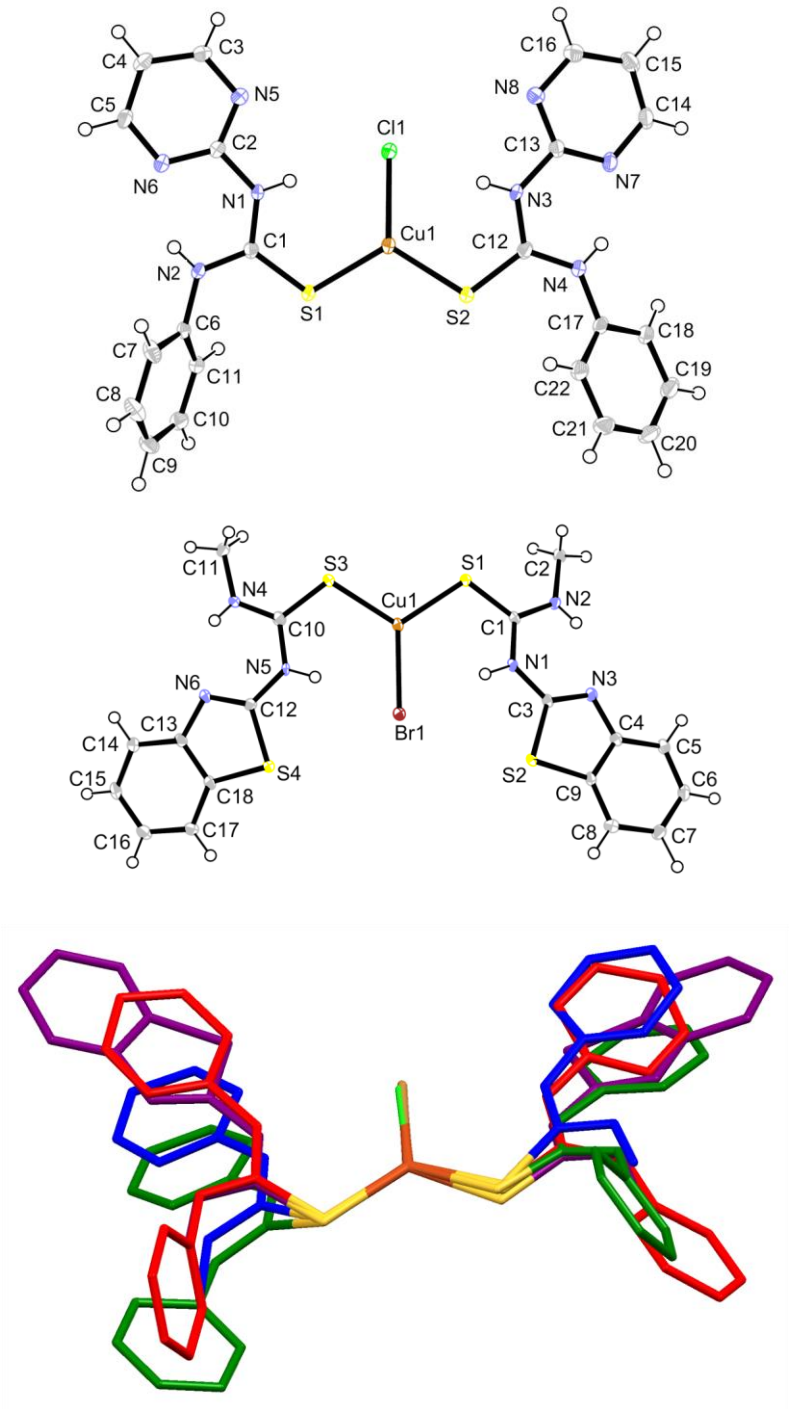


Figure 1. (A) Thermal ellipsoid (50%) drawing of CuCl(**6**)$_2$. (B) Thermal ellipsoid (50%) drawing of CuBr(**9**)$_2$. (B) Overlay of CuCl(**6**)$_2$ (red), CuCl(**7**)$_2$ (blue), CuBr(**6**)$_2$ (green), and CuBr(**9**)$_2$ (purple). Central plane atom colors: S = yellow, Cu = orange, Cl = lime green, Br = brown.

The second category of monomer includes nitrate complexes with potentially chelating HetTu ligands. The sole representative of this class in the current study was [Cu(**10**)$_2$]NO$_3$. However, [Cu(**10**)$_2$]NO$_3$ is directly analogous to the previously reported [Cu(**10**)$_2$]ClO$_4$ [7]. The nitrate complex consists of a 4-coordinate copper(I) tetrahedrally chelated to S and $N_{Py}$ from two ligands, see Figure 2. The nitrate ion is non-coordinating. Although this cation is analogous to that previously seen for the perchlorate ion [7], in the current case the S–Cu–S bond angle is much more open (129.35(2)$^o$ vs. 119.85(7)$^o$, respectively). This larger angle comes at the expense of a more constricted S–Cu–N (115.55(4)$^o$ vs. 120.6(1)$^o$) and N–Cu–N (109.15(6)$^o$ vs. 115.6(2)$^o$). The non-coordinated $N_{Py}$ (N4, N8) on each ligand engages in intramolecular hydrogen-bonding with a thiourea N–H (N1, N5). The remaining thiourea N–H on each ligand (N3, N7) hydrogen-bonds to the nitrate ion, producing a 1D chain (Figure S1). The 1:2 stoichiometry seen for [Cu(**10**)$_2$]NO$_3$ was in agreement with that of the bulk product.

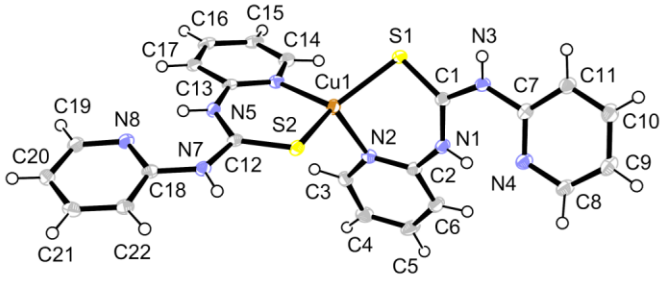


Figure 2. Thermal ellipsoid (50%) drawing of [Cu(**10**)$_2$]NO$_3$. The nitrate counterion is omitted.

*3.1.2. Polymeric Complexes ($I^0O^1$)*

Closely related to the four halide 1:2 monomers described above is CuBr(**1**)$_2$, which is depicted in Figure 3. The difference is the addition of SAB behavior by HetTu sulfur atom, S2. This bridging increases the copper center to 4-coordinate and produces a 1D $I^0O^1$-type [3] zigzag polymer chain having a ···Cu–S–Cu–S··· backbone. The chain propagates in parallel direction to the crystallographic *a*-axis. Although one of the two Cu1–S2 bonds is about 0.2 Å longer than the

other two Cu–S bonds, the bond angles around Cu reflect approximately tetrahedral geometry, confirming 4-coordination. As with the monomeric structures described above, the heterocycle ring nitrogen (N3, N6) on each ligand does not interact with copper, but instead forms an intramolecular hydrogen-bond with a HetTu N–H (N2, N5). Also in like fashion to the $CuX(HetTu)_2$ monomers, approximate coplanarity is found between the thiourea planes (less Cu, which is displaced), and the planes of the heterocycles are oriented toward the Br. Very weak π-stacking (centroid···centroid = 4.036 Å) occurs between symmetry-related, non-coordinating pyridyl rings on adjacent ligands. The bulk product of CuBr with **1** does not show 1:2 stoichiometry (see Table 1).

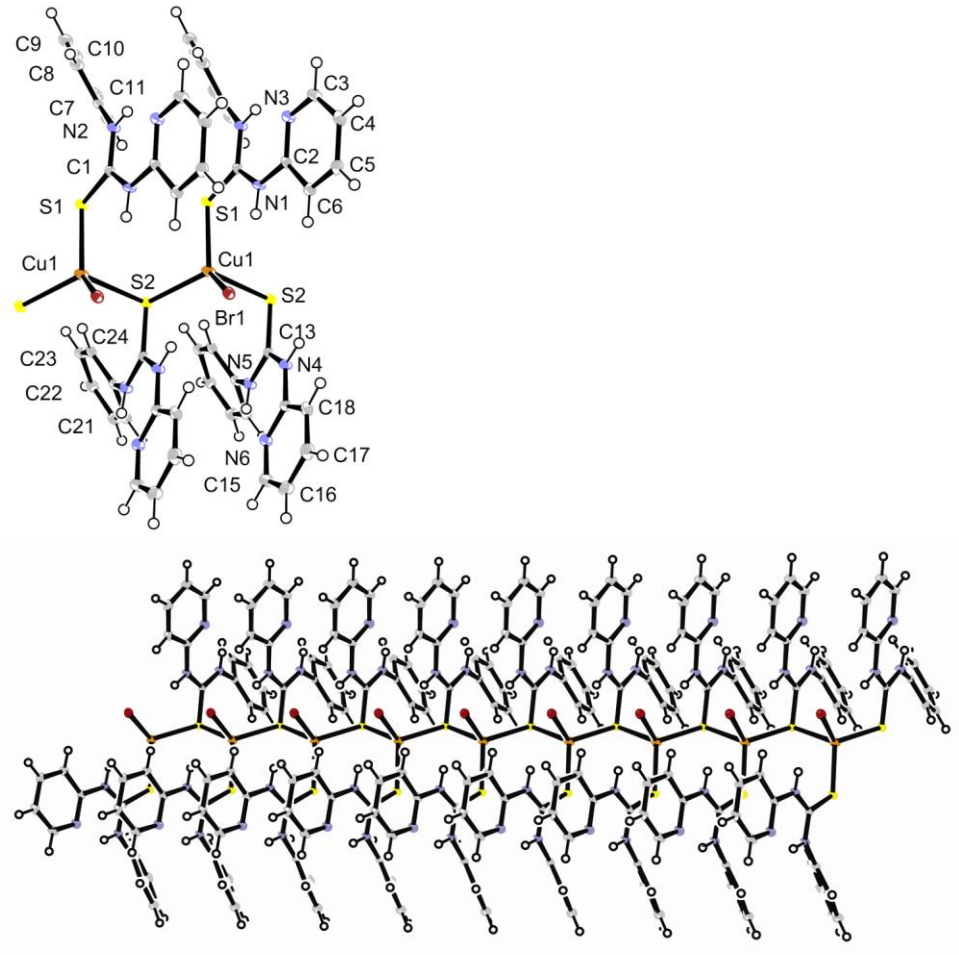


Figure 3. Thermal ellipsoid (50%) drawings of $CuBr(\mathbf{1})_2$. A: Repeat unit with atomic numbering. B: The long-range chain arrangement.

The nitrate complex $[Cu(\mathbf{3})_2]NO_3$ is a HetTu-bridged 1D polymer (Figure 4). It is instructive to compare $[Cu(\mathbf{3})_2]NO_3$ to $[Cu(\mathbf{10})_2]NO_3$ (see above), which have identical stoichiometry and analogous connectivity. In contrast to the 2-pyridyl HetTu ligands of **10**, 3-pyridyl ligands cannot chelate; instead they bridge metal centers. Both thiourea ligands in $[Cu(\mathbf{3})_2]^+$ bridge pairs of 4-coordinate copper centers in a κS:N fashion (Figure 4A). The resulting dimers share copper centers, resulting in an $I^0O^1$ chain-link polymer propagating in the crystallographic *b*-direction (Figure 4B). π-Stacking is evident between symmetry-related pyridyl rings that bridge pairs of Cu atoms (centroid···centroid = 3.618 Å). Since both pyridyl nitrogen atoms coordinate to copper, no intramolecular thiourea hydrogen-bonding is possible. Instead, the nitrate oxygens act as hydrogen-bond donors for three thiourea N–H units. The nitrate ions sit in grooves along the metal-organic chain, linking adjacent thiourea ligands (N1–H···O3, N4–H···O1, N5–H···O2) within the chain (see Figure S2). Hydrogen-bonding to nitrate causes N4/N5 in this **3** ligand to adopt a Z,Z conformation [6], a unique occurance in the current study and the direct result of the lack of the internal hydrogen-bonds. Disordered acetone molecules (1.5 per Cu) were found lying between the metal-organic ribbons. These solvent molecules were removed using Platon SQUEEZE [11] to improve the structure quality (removed volume per unit cell = 328.4 $Å^3$). The bulk product of $CuNO_3$-**3** is of different stoichiometry than that of the crystal structure.

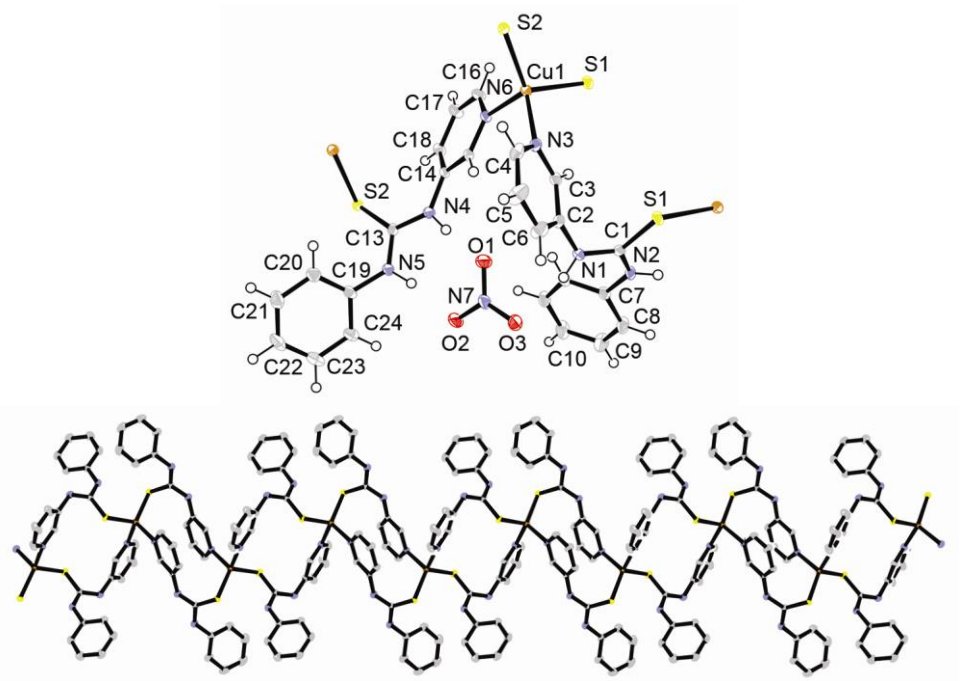


Figure 4. Thermal ellipsoid (50%) drawing of [Cu(**3**)$_2$]$NO_3$. Acetone molecules removed using Platon Squeeze. A: Repeat unit with atomic numbering. B: The long-range chain-link arrangement. Nitrate ion and hydrogen atoms are omitted.

*3.1.3. Polymeric Complexes ($I^{0.5}O^{0.5}$)*

Two closely related 1:1 CuI:HetTu structures were solved: CuI(**7**) and CuI(**9**). The 1:1 ratio of the former, but not of the latter, is in agreement with that of the bulk product. Both structures are composed of 4-coordinate Cu centers alternately bridged by pairs of iodide ions and pairs of thiocarbonyl sulfur atoms, acting as SABs. The resulting 1D ribbons consist of corner-sharing $Cu_2I_2$ and $Cu_2S_2$ rings propagating parallel to the crystallographic *b*-direction. Since a single polymeric strand is produced through the bridging of both inorganic and organic SABs, it seems appropriate to label this sort of networking $I^{0.5}O^{0.5}$. Although structures with copper-sharing $(Cu_2X_2)_\infty$ [12] or $(Cu_2S_2)_\infty$ chains [5] are fairly common, the alternating arrangement $(Cu_2X_2Cu_2S_2)_\infty$ seen in the following two structures is very unusual, having been reported only once previously [13].

In CuI(**9**) (Figure 5), there are single crystallographically-unique Cu, I, and HetTu units. Therefore, the corner-sharing $Cu_2I_2$ and $Cu_2S_2$ rings are rigorously planar. These planes are nearly mutally perpendicular (interplanar angle = 84.4°). An intramolecular N1–H···N3 hydrogen-bond is present in the **9** ligand and the benzothiazole group is nearly coplanar with the thiourea core. The Cu···Cu distance in the $Cu_2I_2$ unit is just under the van der Waals sum of 2.8 Å (2.719(2) Å), and for $Cu_2S_2$, the Cu···Cu is slightly larger (3.017(2) Å). There is no interaction between the heterocyclic rings in CuI(**9**).

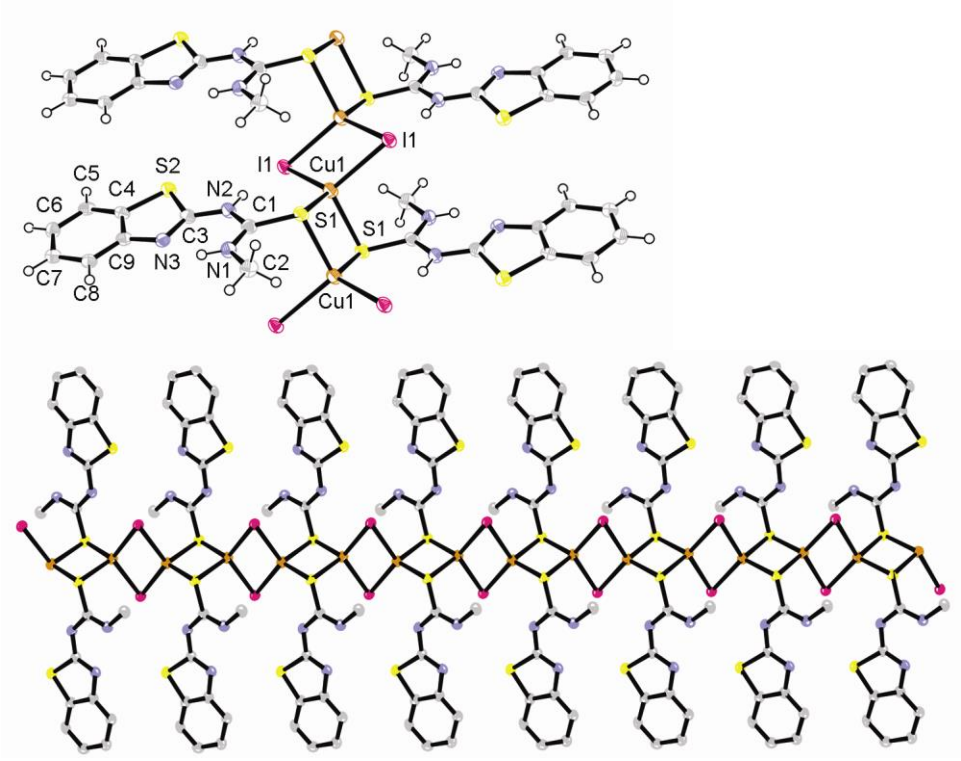


Figure 5. Thermal ellipsoid (50%) drawings of CuI(**9**). A: Repeat unit with atomic numbering. B: The long-range chain-link arrangement. Hydrogen atoms are omitted.

In like fashion to CuI(**9**), CuI(**7**) shows corner-sharing $Cu_2I_2$ and $Cu_2S_2$ rings propagating parallel to the crystallographic *b*-direction (Figure 6). In contrast however, the pyrimidyl rings in CuI(**7**) are noticeably inclined toward one another to allow π-stacking (centroid···centroid = 3.552 Å). This results in significant puckering of the rings and a slightly wavy chain. There are two

crystallographically-independent Cu, I, and HetTu in this structure. The $Cu_2I_2$ and $Cu_2S_2$ rings are both puckered, with maximum atom RMS deviations from best-fit planarity of 0.1871 and 0.0699 Å, respectively. The best planes for $Cu_2I_2$ and $Cu_2S_2$ show an interplanar angle of 85.64(2)°. The two **7** ligands are nearly coplanar (interplanar angle = 4.1(1)°). Near-van der Waals Cu···Cu interactions across the $Cu_2I_2$ and $Cu_2S_2$ rhombs of 2.7927(9) and 2.9349(9) Å are seen. An intramolecular N1–H···N4 hydrogen-bond is noted between the coplanar Pym ring and the HetTu core.

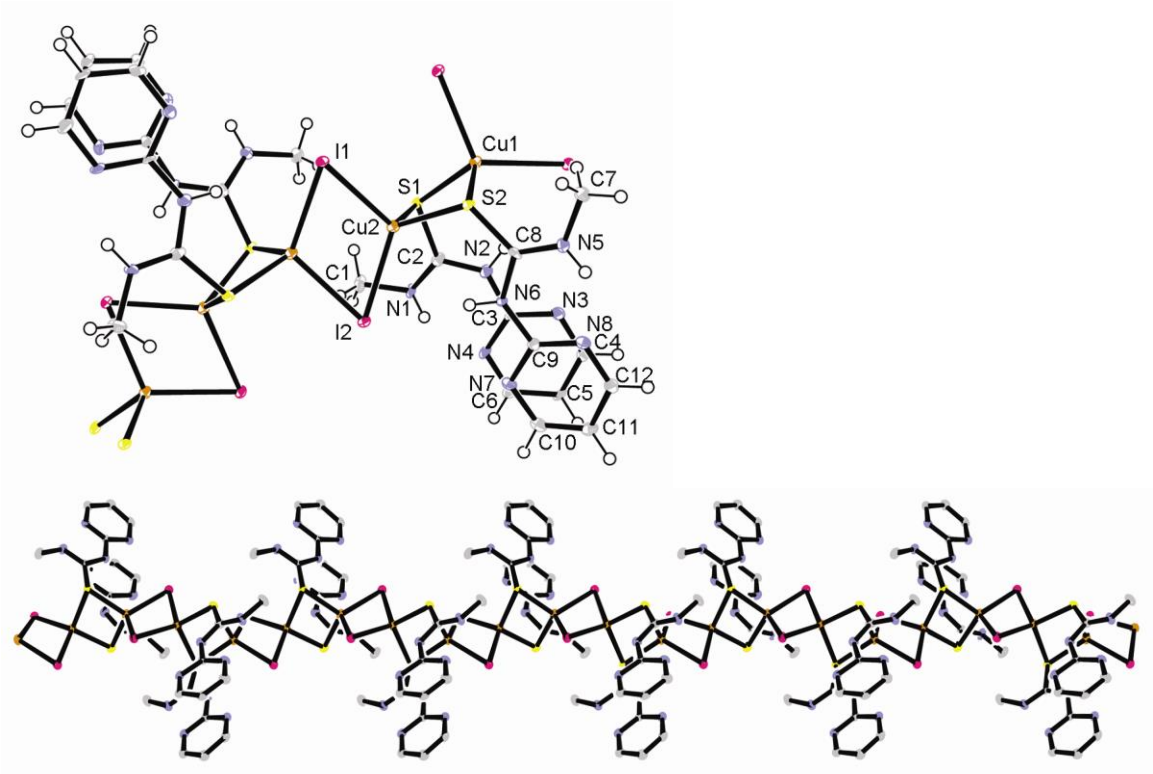


Figure 6. Thermal ellipsoid (50%) drawings of CuI(**7**). A: Repeat unit with atomic numbering. B: The long-range chain-link arrangement. Hydrogen atoms are omitted.

*3.1.4. Sheet Complex ($I^1O^1$)*

The structure of CuCl(**10**) features the HetTu bridging in a κS:N fashion, as was described above for $[Cu(\mathbf{3})_2]NO_3$ (Figure 7). Ligand **10**, which was seen to chelate in both

[Cu(**10**)$_2$]ClO$_4$ [7] and [Cu(**10**)$_2$]NO$_3$ (see above), acts as a network-former here. The structure of CuCl(**10**) features the $Cu_2Cl_2$ rhomboid dimers, akin to the $Cu_2I_2$ units in CuI(**9**) and CuI(**7**). One crystallographically-independent Cu, Cl and HetTu are present. Each 4-coordinate copper center is also coordinated by a sulfur atom and an $N_{Py}$ from separate HetTu ligands (Figure 7A). As a result, the **10** ligands bridge the $Cu_2Cl_2$ units, creating $(Cu_2Cl_2)_4$(**10**)$_4$ rings, which are tiled together into a 2D $I^1O^1$ sheet running in the *a,b* plane (Figure 7B). The Cu···Cu distance in the $Cu_2Cl_2$ unit is greater than the van der Waals sum of 2.8 Å (3.0049(5) Å), suggesting a lack of significant metal–metal bonding. The expected N2–H···N3 and N1–H···Cl1 H-bonds are found. As a result of the latter interaction, the N3-bearing ring is roughly coplanar with the NC(S)N plane. The bulk CuCl-**10** product shows 2:3 stoichiometry.

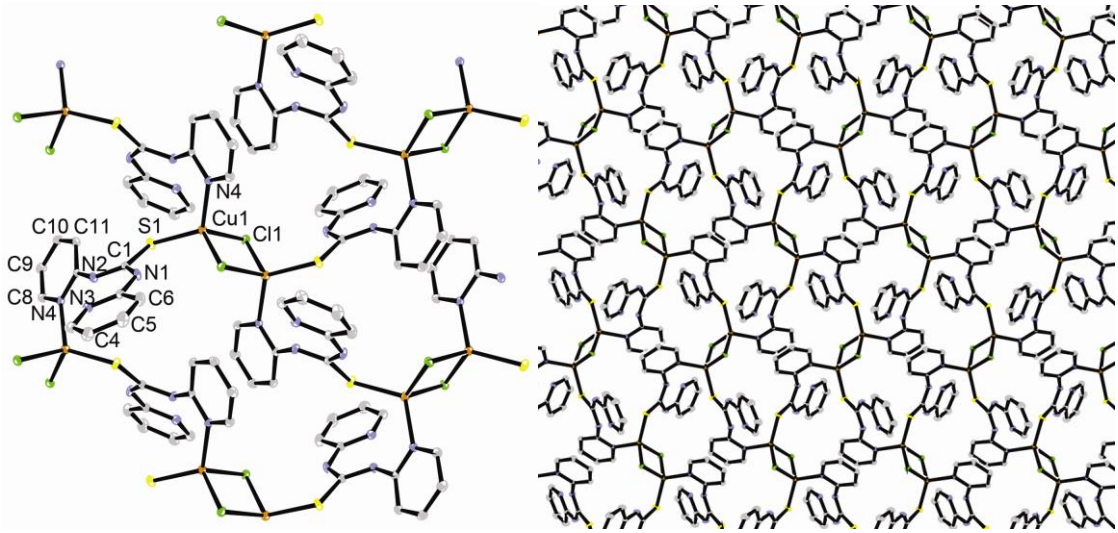


Figure 7. Thermal ellipsoid (50%) drawings of CuCl(**10**). Hydrogen atoms are omitted. A: Repeat unit with atomic numbering. B: The long-range sheet arrangement.

*3.1.5. Cyclized Ligand Complexes*

The final two structures show ligand reconstruction. Crystallization of a CuI-**6** mixture resulted in a CuI complex of N-(pyrimidin-2-yl)benzo[d]thiazol-2-amine (**12**, Scheme 1). The

copper iodide network arrangement within the structure of $[(CuI)_2(\mathbf{12})]\bullet 2CH_3CN$ is interesting in its own right (Figure 8). Two half-independent and one fully-independent 4-coordinate copper atoms are present. They are bridged by two fully-independent $\mu_3$-iodine atoms to form a modified stair-step pattern. As shown in Chart 3, a conventional stair-step pattern (whether truncated [14] or infinite [4,15]) is produced when $Cu_2X_2$ rings share opposite edges. Conventional stair-step chains propagate in a single crystallographic direction. The metal centers may be decorated with monodentate ligands, chelated by bidentate ligands ($I^1O^0$) [14], or multiple chains may be crosslinked with bridging ligands ($I^1O^1$) [4,15]. In the case of infinite stair-step structures, all copper atoms feature $CuX_3L$ coordination. Uniquely in the current structure, the infinite stair-step ribbons show a zigzag structure, see Figure 8B. Bond distances for Cu–I are fairly consistent, suggesting a true stair-step configuration, rather than a sequence of weakly interacting dimers. As illustrated in Chart 3, sequences of five opposite edge-sharing $Cu_2I_2$ rings are linked by adjacent edge-sharing. Forming each "corner" $Cu_2I_2$ unit are two half-independent copper atoms having $CuI_2L_2$ and $CuI_4$ coordination (Cu1 and Cu3, respectively). The linear section of the chain is formed by opposite edge-sharing Cu1/I1/Cu3/I2 and Cu2/I2/Cu2/I2 units. Close Cu···Cu interactions across the $Cu_2X_2$ rings measuring 2.694(1) and 2.722(1) Å are noted for Cu2···Cu2 and Cu1···Cu3. Since both iodide and **12** ligands participate in formation of a 1D structure, we will classify the networking in $[(CuI)_2(\mathbf{12})]$ as $I^{0.5}O^{0.5}$.

Scheme 1

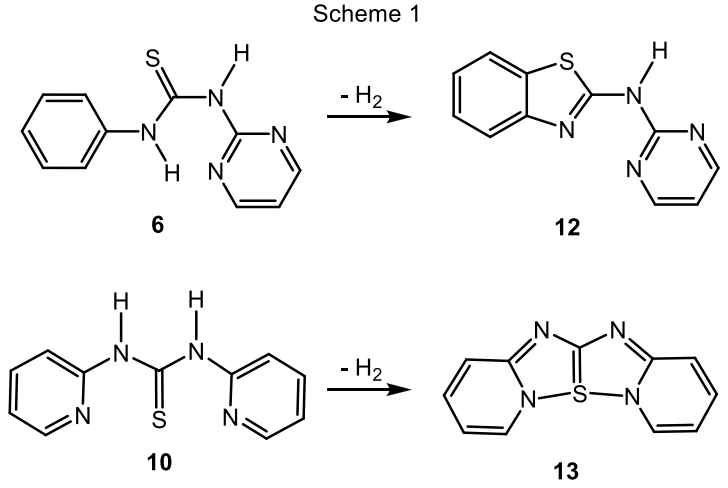

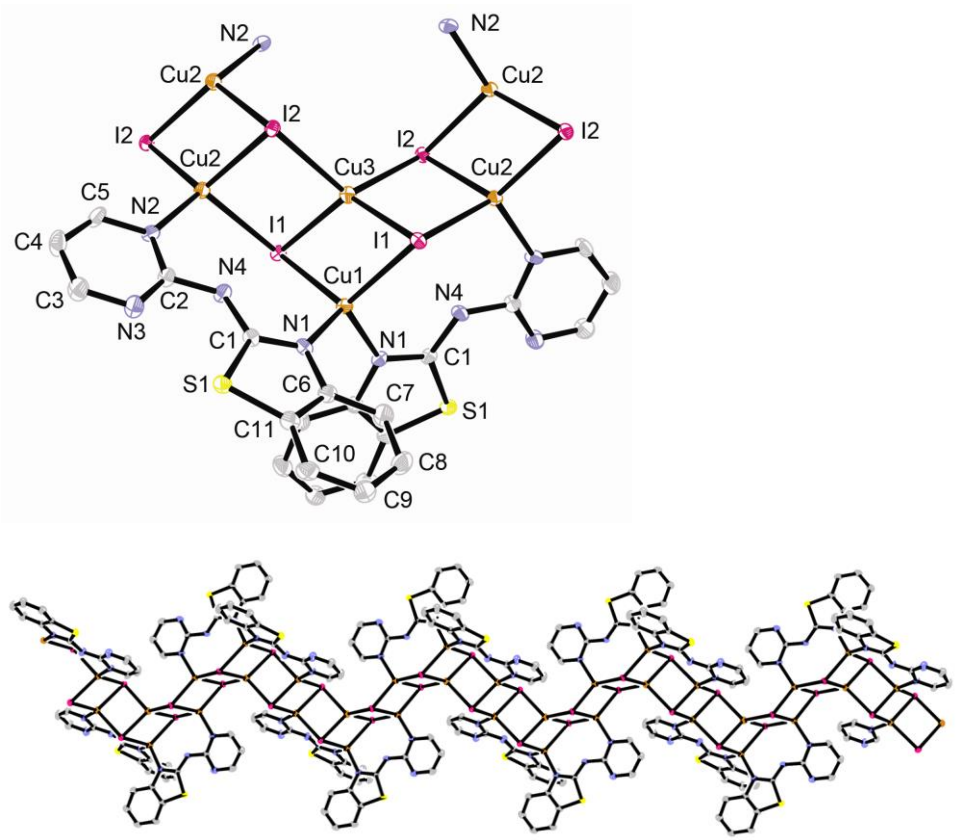


Figure 8. Thermal ellipsoid (50%) drawings of $[(CuI)_2(\mathbf{12})]\bullet 2CH_3CN$. A: Repeat unit with atomic numbering. B: The long-range stair-step arrangement. The disordered $CH_3CN$ is omitted.

Chart 3

Conventional Stair-Step

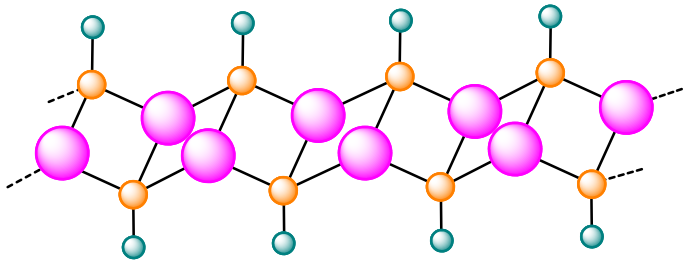

$(CuI)_2$(**12**)

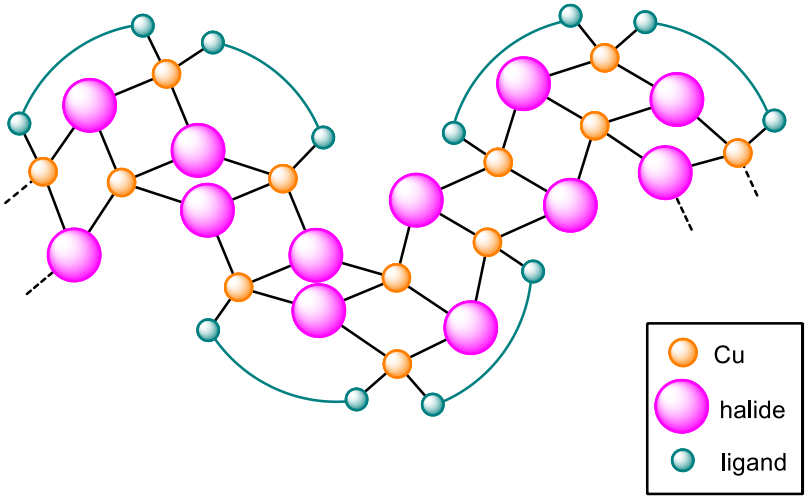


The ligand has undergone an oxidative cyclization **6** → **12** (Scheme 1), converting the phenylthioamide portion into a benzothiazole, with the pyrimdyl ring remaining unaffected. The two rings in the single independent **12** ligand are nearly coplanar (interplanar angle = 2.2(2)°). They coordinate to the metal atoms in bridging fashion through one nitrogen atom on each of the rings, with a pair of ligands lying alongside each linear section of the zigzag stair-step. As is the case for the CuI(**9**) structure, the sulfur atoms in the heterocyclic ring do not coordinate. A disordered half molecule $CH_3CN$ of crystallization is also present.

When a solution of **10** in acetone was layered with a $CuNO_3/CH_3CN$ solution, two different crystalline products formed in approximately equal proportions. While the orange blocks proved to be the expected monomeric [Cu(**10**)$_2$]$NO_3$ described above, the yellow blades yielded a surprising dinuclear structure: [$Cu_2(NO_3)$(**13**)$_2$(MeCN)]$NO_3$ (**13** = dipyridyltetraazathiapentalene

[16]), Figure 9. The structure of the unusual **13** molecule is known [17]. It has previously been prepared via the reaction of 2-aminopyridine with carbon disulfide under air. Thus, in the present case, the oxidation of some free **10** to **13** most likely took place during the week-long crystallization experiment (Scheme 1).

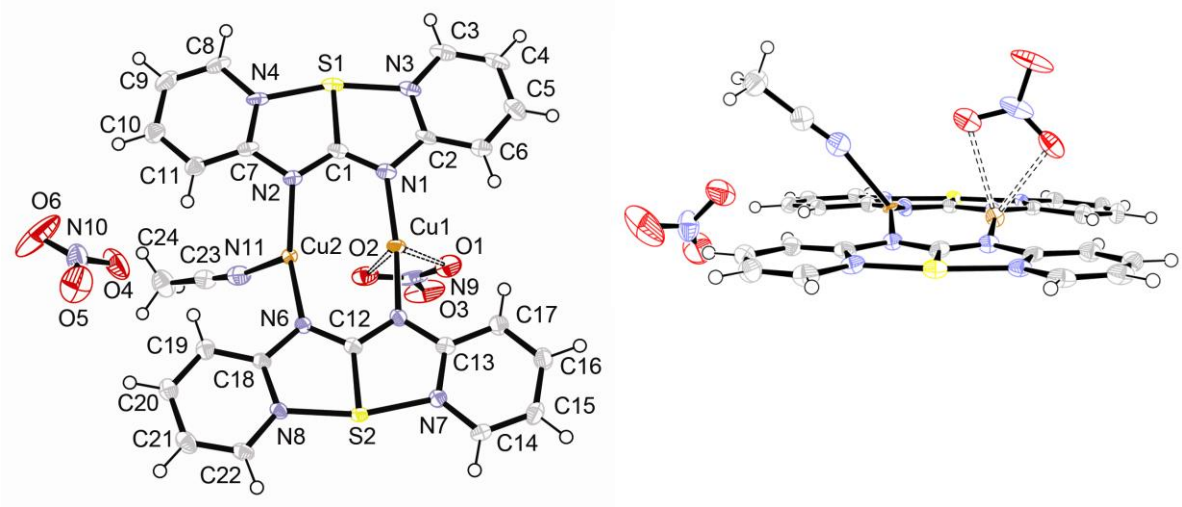


Figure 9. Thermal ellipsoid (50%) drawings of $[Cu_2(NO_3)(\mathbf{13})_2(MeCN)]NO_3$, two views.

The dinuclear structure shown in Figure 9 represents the first reported metal complex of **13**. The bond lengths within the ligand are only slightly altered from those of the free ligand, see Table 4. The major structural difference noted in **13** upon coordination is that the two S–N bonds become much more alike, suggesting greater π-bond delocalization. It acts as a bidentate, bridging ligand through a pair of nitrogen atoms lying on the same side of the ring system. As has been noted with the other thiazole ligands in this study, the ring sulfur atoms do not coordinate. Both **13** ligands are relatively planar, the S1-bearing ring being slightly more so. The maximum RMS deviation from planarity in the S1 ring is 0.0430(5) Å for C6, while that in the S2 ring is 0.119(5) Å for C16. The two ligands are almost mutually coplanar (interplanar angle = 6.46(6)°).

Given the neutral charge of **13** and the presence of two nitrate ions in the structure, both copper atoms are clearly Cu(I). This conclusion is also supported by the Cu coordination

geometries. Atom Cu1 shows approximately linear coordination with two **13** nitrogen atoms (N1–Cu1–N5 = 164.0(2)°). However, it is also weakly bonded to a nitrate atom in chelating fashion (Cu1···O1 = 2.341(4), Cu1···O2 = 2.588(5) Å). Atom Cu2 shows slight positional disorder. Its major position is elevated slightly from the ligand planes. However, there is a second weaker center of electron density about 0.23 Å beneath primary Cu2 site, lying roughly in the plane. The coordination environment of Cu2 can be described as approximately trigonal planar, with coordination to two nitrogens from **13** and one from MeCN. However, the nominally trigonal N2–Cu2–N6 angle is quite large (152.3(3)°). The remaining nitrate in the crystal structure is neither coordinated nor hydrogen-bonded to the cation. There is a rather close Cu···Cu interaction of 2.672(7) Å which is certainly the result of the dinuclear bridging arrangement forced by **13**.

## 4. Conclusions

The preparation of CuCl, CuBr, CuI, and $CuNO_3$ complexes of various HetTu thiourea ligands has produced a variety of product stoichiometries and structural types, including both monomeric and polymeric species. Product CuX:HetTu stoichiometries ranged from 1:1 to 1:5, with 1:1, 2:3, and 1:2 being most common. These relatively copper-rich products are polymeric or networked in some cases. The marked tendency for stoichiometrically distinct products to result from bulk synthesis versus slow crystal growth experiments emphasizes a propensity toward variable product formulations. The full extent of this trend was not explored herein.

This study was undertaken with the intent of using the potentially polydentate HetTu ligands to produce highly networked MONs containing Cu(I). Therefore, it was surprising that simple, 3-coordinate $CuX(HetTu)_2$ monomers were found in so many of the structures. The versatility of the HetTu species as polydentate ligands appears to be offset by several factors: (1) the relatively weak donor ability of aromatic nitrogen atoms, (2) the relatively large size of the HetTu ligands, (3) their proclivity to tie up lone pairs through internal hydrogen-bond formation,

and (4) a tendency toward ligand oxidative cyclization. Finally, the copper(I) ion's willingness to remain 3-coordinate works against network formation.

Nevertheless, HetTu ligands were sometimes found to act as network-formers. In such cases HetTu bridging was accomplished via coordination of the thiourea sulfur atom and a ring nitrogen atom. In addition, the well-known SAB behavior of thiourea sulfur and/or halide (particularly iodide) was seen, resulting in polymer or network formation. An overall bonding preference: thiocarbonyl S ~ halide > heterocycle N > nitrate >> heterocycle S, thiourea N was noted for Cu(I).

**5. Supplementary Material:** Tables of hydrogen bonds and interplanar angles, and hydrogen-bonding pictures. Appendices A–L (CCDC 734325–734336) contain the supplementary crystallographic data for all structures. These data can be obtained free of charge via http://www.ccdc.cam.ac.uk/conts/retrieving.html, or from the Cambridge Crystallographic Data Centre, 12 Union Road, Cambridge CB2 1EZ, UK; fax: (+44) 1223-336-033; or e-mail: deposit@ccdc.cam.ac.uk.

**Acknowledgement.** This research was supported in part by donors of the American Chemical Society Petroleum Research Fund (44891-B3). We are indebted to NSF (CHE-0443345) and the College of William and Mary for the purchase of the X-ray equipment.

**References**

[1] (a) C. Janiak, Dalton Trans. (2003) 2781; (b) P.M. Forster, A.K. Cheetham, Top. Catal. 24 (2003) 79; (c) B. Kesanli, W. Lin, Coord. Chem. Rev. 246 (2003) 305; (d) U. Muller, M. Schubert, F. Teich, H. Puetter, K. Schierle-Arndt, J. Pastré, J. Mater. Chem. 16 (2006) 626; (e) M. Dincă, A.F. Yu, J.R. Long, J. Am. Chem. Soc. 128 (2006) 8904; (f) A.K.

Cheetham, C.N.R. Rao, R.K. Feller, Chem. Commun. (2006) 4780; (g) J.A. Brant, Y. Liu, D.F. Sava, D. Beauchamp, M. Eddaoudi, J. Molec. Struct. 796 (2006) 160.

[2] J.Y. Lu, Coord. Chem. Rev. 246 (2003) 327.

[3] A.K. Cheetham, C.N.R. Rao, R.K. Feller, Chem. Commun. (2006) 4780.

[4] P.M. Graham, R.D. Pike, M. Sabat, R.D. Bailey, W.T. Pennington, Inorg. Chem. 39 (2000) 5121.

[5] (a) F. Hanic, E. Durcanska, Inorg. Chim. Acta 3 (1969) 293; (b) W.A. Spofford, E.L. Amma, Acta Crystallogr., Sect. B 26 (1970) 1474; (c) I.F. Taylor, M.S. Weininger, E.L. Amma, Inorg. Chem. 13 (1974) 2835; (d) M.B. Ferrari, G.F. Gasparri, Cryst. Struct. Commun. 5 (1976) 935; (e) G.W. Hunt, N.W. Terry, E.L. Amma, Acta Crystallogr., Sect. B 35 (1979) 1235; (f) M. van Meerssche, R. Kamara, J.P. Declercq, G. Germain, Bull. Soc. Chim. Belg. 91 (1982) 547 (g) E. Dubler, W. Bensch, Inorg. Chim. Acta 125 (1986) 37; (h) E.S. Raper, J.D. Wilson, W. Clegg, Inorg. Chim. Acta 194 (1992) 51; (i) C. Palivan, T. Berclaz, M. Geoffroy, S. Ramaprabhu, G. Bernardinelli, J. Chem. Soc., Faraday Trans. 91 (1995) 2155; (j) R.C. Bott, G.A. Bowmaker, C.A. Davis, G.A. Hope, B.E. Jones, Inorg. Chem. 37 (1998) 651; (k) O.E. Piro, R.C.V. Piatti, A.E. Bolzan, R.C. Salvarezza, A.J. Arvia, Acta Crystallogr., Sect. B 56 (2000) 993; (l) P. Bombicz, I. Mutikainen, M. Krunks, T. Leskela, J. Madarasz, L. Niinisto, Inorg. Chim. Acta 513 (2004) 357; (m) T.S. Lobana, R. Sharma, R. Sharma, S. Mehra, A. Castineiras, P. Turner, Inorg. Chem. 44 (2005) 1914; (n) S. Athimoolam, J. Kumar, V. Ramakrishnan, R.K. Rajaram, Acta Crystallogr., Sect. E 61 (2005) m2014; (o) T.S. Lobana, R. Sharma, G. Hundal, R.J. Butcher, Inorg. Chem. 45 (2006) 9402; (p) M. Mufakkar, S. Ahmad, I.U. Khan, H.-K. Fun, S. Chantrapromma, Acta Crystallogr., Sect. E 63 (2007) m2384; (q) D. Jia, Y. Zhang, J. Deng, M. Ji, J. Coord. Chem. 60 (2007) 833.

[6] A. Saxena, R.D. Pike, J. Chem. Cryst. 37 (2007) 755, and references cited therein.

[7] Y. Fan, H. Lu, H. Hou, Z. Zhou, Q. Zhao, L. Zhang, F. Cheng, J. Coord. Chem. 50 (2000) 65.

[8] SAINT PLUS: Bruker Analytical X-ray Systems: Madison, WI, 2001.

[9] SADABS: Bruker Analytical X-ray Systems: Madison, WI, 2001.

[10] G.M. Sheldrick, Acta Crystallogr., Sect. A 64 (2008) 112.

[11] P.v.d. Sluis, A.L. Spek, Acta Crystallogr., Sect. A 46 (1990) 194.

[12] See for example P.M. Graham, R.D. Pike, M. Sabat, R.D. Bailey, W.T. Pennington, Inorg. Chem. 39 (2000) 5121; (b) J.T. Maeyer, T.J. Johnson, A.K. Smith, B.D. Borne, R.D. Pike, W.T. Pennington, M. Krawiec, A.L. Rheingold, Polyhedron 22 (2003) 419; (c) R.D. Pike, B.A. Reinecke, M.E. Dellinger, A.B. Wiles, J.D. Harper, J.R. Cole, K.A. Dendramis, B.D. Borne, J.L. Harris, W.T. Pennington, Organometallics 23 (2004) 1986.

[13] K. Schulbert, R. Mattes, Z. Naturforsch. 48b (1993) 1227.

[14] (a) R.-F. Song, Y.-B. Xie, J.-R. Li, X.-H. Bu, CrystEngComm. 7 (2005) 249; (b) E. Cariati, D. Roberto, R. Ugo, P.C. Ford, S. Galli, A. Sironi, Inorg. Chem. 44 (2005) 4077; (c) C.-S. Lee, C.-Y. Wu, W.-S. Hwang, J. Dinda, Polyhedron 25 (2006) 1791; (d) R. Peng, D. Li, T. Wu, X.-P. Zhou, S.W. Ng, Inorg. Chem. 45 (2006) 4035; (e) Y.-B. Xie, Z.-C. Ma, D. Wang, J. Mol. Struct. 784 (2006) 93; (f) Z.-C. Ma, H.-S. Xian, J. Chem. Cryst. 36 (2006) 129; (g) J. Diez, M.P. Gamasa, M. Panera, Inorg. Chem. 45 (2006) 10043; (h) C. Ganesamoorthy, M.S. Balakrishna, P.P. George, J.T. Mague, Inorg. Chem. 46 (2007) 848; (i) J. Xiang, Y.-G. Yin, P. Mei, Inorg. Chem. Commun. 10 (2007) 1168; (j) U. Vogel, J.F. Nixon, M. Scheer, Chem. Commun. (2007) 5055; (k) C. R. Samanamu, P.M. Lococo, W.D. Woodul, A.F. Richards, Polyhedron 27 (2008) 1463.

[15] (a) M. Munakata, T. Kuroda-Sowa, M. Maekawa, A. Honda, S. Kitagawa J. Chem. Soc., Dalton Trans. (1994) 2771; (b) C. N≅ther, I. Jess, Monat. Chem. 132 (2001) 897; (c) C. N≅ther, I. Jess, J. Greve, Polyhedron 20 (2001) 1017; (d) N.S. Persky, J.M. Chow, K.A.

Poschmann, N.N. Lacuesta, S.L. Stoll, S.G. Bott, S. Obrey, Inorg. Chem. 40 (2001), 29; (e) C. N≅ther, I. Jess, H. Studzinski, Z. Naturforsch. 56b (2001) 997; (f) C. N≅ther, M. Wriedt, I. Jess, Z. Anorg. Allg. Chem. 628 (2002) 394; (g) C. N≅ther, I. Jess, J. Solid State Chem. 169 (2002) 103; (h) C. N≅ther, I. Jess, Z. Naturforsch. 57b (2002) 1133; (i) C. N≅ther, M. Wriedt, I. Jess, Inorg. Chem. 42 (2003) 2391; (j) T. Kromp, W.S. Sheldrick, C. N≅ther, Z. Anorg. Allg. Chem. 629 (2003) 45.

[16] R.L.N. Harris, Aust. J. Chem. 25 (1972) 993.

[17] R.-B. Huang, X. Lu, N.-F. Zheng, Y.-S. Zou, S.-L. Deng, H.-P. Zhong, S.-Y. Xie, L.-S. Long, L.-S. Zheng, J. Mol. Struct. 610 (2002), 265.

Table 1. Stoichiometry summary for bulk CuX:HetTu reactions.[a]

| Ligand | CuCl | CuBr | CuI | $CuNO_3$ |
|---|---|---|---|---|
| **1** | 1:2 | 1:1•MeCN (1:2) | 1:1 | 1:1 |
| **2** | 2:3 | 1:1•MeCN | 1:1•MeCN | 1:1•MeCN |
| **3** | 1:4 | 1:2 | 1:1 | 1:1•MeCN (1:2•12acetone) |
| **4** | 1:1 | 1:1 | 1:1 | 2:3 |
| **5** | 1:1 | 1:1 | 1:1 | 2:3 |
| **6** | 1:2 (1:2) | 1:2 (1:2) | 1:1 | 1:1 |
| **7** | 1:4 (1:2) | 1:1 | 1:1 (1:1) | 2:3 |
| **8** | 2:3 | 2:3 | 1:1 | 1:2 |
| **9** | 1:1•2MeCN | 1:1 (1:2) | 2:3 (1:1) | 1:1•MeCN |
| **10** | 2:3 (1:1) | 1:1 | 1:1 | 2:3•MeCN[b] |
| | | | | 1:2[c] (1:2) |
| **11** | 1:4 | 1:5 | 1:4 | 1:1•MeCN |

[a]Results for crystal structures in parentheses. [b]One hour reaction result. [c]Four hour reaction result.

Table 2. Crystal and Structure Refinement Data.

| complex | CuCl(**6**)$_2$ | CuCl(**7**)$_2$ | CuBr(**6**)$_2$ |
|---|---|---|---|
| CCDC deposit no. | 734330 | 734329 | 734327 |
| color and habit | colorless prism | colorless block | colorless blade |
| size, mm | 0.20 × 0.11 × 0.06 | 0.23 × 0.14 × 0.10 | 0.23 × 0.08 × 0.03 |
| formula | $C_{22}H_{20}ClCuN_8S_2$ | $C_{12}H_{16}ClCuN_8S_2$ | $C_{22}H_{20}BrCuN_8S_2$ |
| formula weight | 559.57 | 435.44 | 604.03 |
| space group | *P*–1 (#2) | *P*–1 (#2) | $P2_1/c$ (#14) |
| *a*, Å | 9.0220(3) | 9.1759(3) | 16.0707(2) |
| *b*, Å | 9.6852(3) | 9.2899(3) | 9.8486(2) |
| *c*, Å | 15.2802(5) | 10.6780(4) | 15.8994(2) |
| α, deg | 106.042(2) | 88.259(2) | 90 |
| β, deg | 95.231(2) | 73.034(2) | 107.2950(10) |
| γ, deg | 107.933(2) | 80.515(2) | 90 |
| volume, Å$^3$ | 1197.95(7) | 858.56(5) | 2402.68(6) |
| Z | 2 | 2 | 4 |
| $\rho_{calc}$, g cm$^{-3}$ | 1.551 | 1.684 | 1.670 |
| $F_{000}$ | 572 | 444 | 1216 |
| μ(Cu Kα), mm$^{-1}$ | 4.178 | 5.619 | 5.092 |
| temperature, K | 100 | 100 | 100 |
| residuals:[a] R; $R_w$ | 0.0269; 0.0707 | 0.0300; 0.0775 | 0.0237; 0.0650 |
| goodness of fit | 1.058 | 1.037 | 1.039 |

[a]$R = R_1 = \Sigma||F_o| - |F_c||/ \Sigma|F_o|$ for observed data only. $R_w = wR_2 = \{\Sigma[w(F_o^2 - F_c^2)^2]/\Sigma[w(F_o^2)^2]\}^{1/2}$ for all data. [b]Full formula = [Cu(**3**)$_2$]$NO_3$•1.5acetone; solvent molecules removed with Platon SQUEEZE [11].

Table 2. Cont'd.

| complex | CuBr(**9**)$_2$ | [Cu(**10**)$_2$]$NO_3$ | CuBr(**1**)$_2$ |
|---|---|---|---|
| CCDC deposit no. | 734326 | 734334 | 734325 |
| color and habit | colorless blade | orange plate | yellow prism |
| size, mm | 0.28 × 0.05 × 0.02 | 0.23 × 0.20 × 0.07 | 0.24 × 0.08 × 0.05 |
| formula | $C_{18}H_{18}BrCuN_6S_4$ | $C_{22}H_{20}CuN_9O_3S_2$ | $C_{24}H_{22}BrCuN_6S_2$ |
| formula weight | 590.07 | 586.13 | 602.05 |
| space group | $P2_1/n$ (#14) | $P\bar{1}$ (#2) | $P2_1/c$ (#14) |
| *a*, Å | 8.39470(10) | 8.9185(3) | 3.89670(10) |
| *b*, Å | 6.12200(10) | 10.5834(4) | 21.4501(4) |
| *c*, Å | 42.6876(4) | 14.2417(5) | 28.1167(5) |
| α, deg | 90 | 68.983(2) | 90 |
| β, deg | 90.5200(10) | 83.742(2) | 91.0940(10) |
| γ, deg | 90 | 75.018(2) | 90 |
| volume, Å$^3$ | 2193.73(5) | 1211.97(7) | 2349.69(9) |
| Z | 4 | 2 | 4 |
| $\rho_{calc}$, g cm$^{-3}$ | 1.787 | 1.606 | 1.702 |
| $F_{000}$ | 1184 | 600 | 1216 |
| μ(Cu Kα), mm$^{-1}$ | 7.260 | 3.279 | 5.179 |
| temperature, K | 100 | 100 | 100 |
| residuals:[a] R; $R_w$ | 0.0268; 0.0647 | 0.0274; 0.0762 | 0.0230; 0.0588 |
| goodness of fit | 1.044 | 1.018 | 1.019 |

[a]$R = R_1 = \Sigma||F_o| - |F_c||/\Sigma|F_o|$ for observed data only. $R_w = wR_2 = \{\Sigma[w(F_o^2 - F_c^2)^2]/\Sigma[w(F_o^2)^2]\}^{1/2}$ for all data. [b]Full formula = [Cu(**3**)$_2$]$NO_3$•1.5acetone; solvent molecules removed with Platon SQUEEZE [11].

Table 2. Cont'd.

| complex | $[Cu(\mathbf{3})_2]NO_3$[b] | CuI(**9**) | CuI(**7**) |
|---|---|---|---|
| CCDC deposit no. | 734335 | 734331 | 734333 |
| color and habit | yellow prism | yellow blade | colorless prism |
| size, mm | 0.21 × 0.10 × 0.07 | 0.21 × 0.11 × 0.03 | 0.19 × 0.13 × 0.12 |
| formula | $C_{24}H_{22}CuN_7O_3S_2$ | $C_9H_9CuIN_3S_2$ | $C_{12}H_{16}Cu_2I_2N_8S_2$ |
| formula weight | 584.15 | 413.75 | 717.33 |
| space group | *P*–1 (#2) | $P2_1/c$ (#14) | $P2_1/n$ (#14) |
| *a*, Å | 9.88290(10) | 13.8265(4) | 12.5978(3) |
| *b*, Å | 12.38390(10) | 5.7143(2) | 10.7859(3) |
| *c*, Å | 12.6176(2) | 15.3147(4) | 14.4601(4) |
| α, deg | 92.2580(10) | 90 | 90 |
| β, deg | 98.3810(10) | 93.1450(10) | 90.1420(10) |
| γ, deg | 101.6420(10) | 90 | 90 |
| volume, $Å^3$ | 1492.55(3) | 1208.17(6) | 1964.81(9) |
| Z | 2 | 4 | 4 |
| $\rho_{calc}$, g $cm^{-3}$ | 1.300 | 2.275 | 2.425 |
| $F_{000}$ | 600 | 792 | 1360 |
| μ(Cu Kα), $mm^{-1}$ | 2.640 | 25.640 | 29.469 |
| temperature, K | 100 | 100 | 100 |
| residuals:[a] R; $R_w$ | 0.022; 0.0846 | 0.0397; 0.1128 | 0.0255; 0.0669 |
| goodness of fit | 1.044 | 1.049 | 1.063 |

[a]$R = R_1 = \Sigma||F_o| - |F_c||/ \Sigma|F_o|$ for observed data only. $R_w = wR_2 = \{\Sigma[w(F_o^2 - F_c^2)^2]/\Sigma[w(F_o^2)^2]\}^{1/2}$ for all data. [b]Full formula = $[Cu(\mathbf{3})_2]NO_3$•1.5acetone; solvent molecules removed with Platon SQUEEZE [11].

Table 2. Cont'd.

| complex | CuCl(**10**) | $[(CuI)_2(\mathbf{12})]\bullet 2MeCN$ | $[Cu_2(NO_3)(\mathbf{13})_2(MeCN)]NO_3$ |
|---|---|---|---|
| CCDC deposit no. | 734328 | 734332 | 734336 |
| color and habit | colorless blade | colorless needle | yellow blade |
| size, mm | 0.17 × 0.09 × 0.03 | 0.17 × 0.04 × 0.04 | 0.15 × 0.10 × 0.05 |
| formula | $C_{11}H_{10}ClCuN_4S$ | $C_{25}H_{22}Cu_4I_4N_9S_2$ | $C_{24}H_{19}Cu_2N_{11}O_6S_2$ |
| formula weight | 329.28 | 1274.40 | 748.70 |
| space group | *P*bcn (#60) | *C*2/c (#15) | $P2_1/c$ (#14) |
| *a*, Å | 9.2669(3) | 15.7316(3) | 11.7014(3) |
| *b*, Å | 15.6365(5) | 16.8380(3) | 30.4798(6) |
| *c*, Å | 17.3257(5) | 13.9026(2) | 7.9358(2) |
| α, deg | 90 | 90 | 90 |
| β, deg | 90 | 100.0460(10) | 108.4800(10) |
| γ, deg | 90 | 90 | 90 |
| volume, $Å^3$ | 2510.53(14) | 3626.18(11) | 2684.40(11) |
| Z | 8 | 8 | 4 |
| $\rho_{calc}$, g $cm^{-3}$ | 1.742 | 2.307 | 1.853 |
| $F_{000}$ | 1328 | 2344 | 1512 |
| μ(Cu Kα), $mm^{-1}$ | 5.853 | 30.704 | 3.990 |
| temperature, K | 100 | 100 | 100 |
| residuals:[a] R; $R_w$ | 0.0207; 0.0576 | 0.0266; 0.0666 | 0.0642; 0.1878 |
| goodness of fit | 1.025 | 1.041 | 1.087 |

[a]$R = R_1 = \Sigma||F_o| - |F_c||/\Sigma|F_o|$ for observed data only. $R_w = wR_2 = \{\Sigma[w(F_o^2 - F_c^2)^2]/\Sigma[w(F_o^2)^2]\}^{1/2}$ for all data. [b]Full formula = $[Cu(\mathbf{3})_2]NO_3\bullet 1.5$acetone; solvent molecules removed with Platon SQUEEZE [11].

Table 3. Selected Bond Distances (Å) and Angles (deg).

| | $CuCl(\mathbf{6})_2$ | $CuCl(\mathbf{7})_2$ | $CuBr(\mathbf{6})_2$ |
|---|---|---|---|
| Cu–S | 2.2141(5), 2.2162(5) | 2.2188(5), 2.2247(5) | 2.2142(6), 2.2261(6) |
| Cu–X[a] | 2.2497(5) | 2.2557(6) | 2.3548(4) |
| Cu–N | – | – | – |
| Cu···Cu | – | – | – |
| S–Cu–S | 117.671(18) | 119.64(2) | 113.51(2) |
| X–Cu–X | – | – | – |
| S–Cu–X | 120.021(18), 122.308(18) | 119.75(2), 120.60(2) | 121.31(2), 125.12(2) |
| S–Cu–N | – | – | – |
| N–Cu–X | – | – | – |
| N–Cu–N | – | – | – |
| Cu–S–Cu | – | – | – |
| Cu–X–Cu | – | – | – |

[a]X = Cl, Br, I. [b]X = $ONO_2$. [c]$N_{MeCN}$. [d]Full formula = $[Cu(\mathbf{3})_2]NO_3 \bullet 1.5$acetone; solvent molecules removed with Platon SQUEEZE [11].

Table 3. Cont'd.

| | CuBr(**9**)$_2$ | [Cu(**10**)$_2$]$NO_3$ | CuBr(**1**)$_2$ |
|---|---|---|---|
| Cu–S | 2.2354(7), 2.2374(7) | 2.2178(5), 2.2846(5) | 2.2611(6), 2.3147(6), 2.5169(6) |
| Cu–X[a] | 2.4216(4) | – | 2.4395(3) |
| Cu–N | – | 2.0069(15), 2.0954(15) | – |
| Cu···Cu | – | – | – |
| S–Cu–S | 114.72(3) | 129.354(19) | 105.79(2), 99.96(2), 107.44(2) |
| X–Cu–X | – | – | – |
| S–Cu–X | 122.41(2), 122.65(2) | – | 123.079(18), 114.951(18), 103.579(16) |
| S–Cu–N | – | 101.16(4), 108.53(4), 115.55(4), 91.67(4) | – |
| N–Cu–X | – | – | – |
| N–Cu–N | – | 109.15(6) | – |
| Cu–S–Cu | – | – | 107.44(2) |
| Cu–X–Cu | – | – | – |

[a]X = Cl, Br, I. [b]X = $ONO_2$. [c]$N_{MeCN}$. [d]Full formula = [Cu(**3**)$_2$]$NO_3$•1.5acetone; solvent molecules removed with Platon SQUEEZE [11].

Table 3. Cont'd.

| | [Cu(**3**)$_2$]NO$_3$[d] | CuI(**9**) | CuI(**7**) |
|---|---|---|---|
| Cu–S | 2.2792(4), 2.3100(4) | 2.3185(15), 2.4258(15) | 2.3413(11), 2.4205(11), 2.3244(11), 2.4866(11) |
| Cu–X[a] | – | 2.6142(7), 2.6553(7) | 2.6063(6), 2.6590(6), 2.6071(6), 2.6339(6) |
| Cu–N | 2.0629(13), 2.0751(14) | – | – |
| Cu···Cu | – | 2.7194(17), 3.0171(17) | 2.7935(8), 2.9346(8) |
| S–Cu–S | 115.614(16) | 101.06(5) | 102.85(4), 101.35(4) |
| X–Cu–X | – | 117.87(3) | 113.64(2), 112.78(2) |
| S–Cu–X | – | 119.39(4), 105.77(4), 103.49(4), 107.56(4) | 118.46(3), 109.46(3), 102.91(3), 108.65(3), 117.36(3), 110.13(3), 103.51(3), 111.01(3) |
| S–Cu–N | 118.90(4), 111.48(4), 101.16(4), 106.99(4) | – | – |
| N–Cu–X | – | – | – |
| N–Cu–N | 101.02(5) | – | – |
| Cu–S–Cu | – | 78.94(5) | 74.80(3), 76.38(3) |
| Cu–X–Cu | – | 62.13(3) | 64.075(18), 64.414(18) |

[a]X = Cl, Br, I. [b]X = $ONO_2$. [c]$N_{MeCN}$. [d]Full formula = [Cu(**3**)$_2$]$NO_3$•1.5acetone; solvent molecules removed with Platon SQUEEZE [11].

Table 3. Cont'd.

| | CuCl(**10**) | $[(CuI)_2(\mathbf{12})]\bullet 2MeCN$ | $[Cu_2(NO_3)(\mathbf{13})_2(MeCN)]NO_3$ |
|---|---|---|---|
| Cu–S | 2.2475(4) | – | – |
| Cu–X[a] | 2.4070(4), 2.4251(4) | 2.6367(5), 2.7070(7), 2.7203(5), 2.6042(7), 2.6753(7), 2.7041(5) | 2.341(4),[b] 2.589(5)[b] |
| Cu–N | 2.0642(13) | 2.036(4), 2.053(4) | 1.912(4), 1.916(4), 1.960(8), 1.973(8), 2.104(8)[c] |
| Cu···Cu | 3.0049(5) | 2.7223(13), 2.6936(13) | 2.672(7) |
| S–Cu–S | – | – | – |
| X–Cu–X | 103.099(14) | 115.91(3), 118.66(3), 109.97(2), 96.08(2), 121.97(4), 110.088(8), 97.070(8), 122.51(4) | – |
| S–Cu–X | 108.578(16), 115.840(16) | – | – |
| S–Cu–N | 118.24(4) | – | – |
| N–Cu–X | 109.02(4), 100.85(4) | 114.76(10), 100.06(10), 111.26(11), 107.02(11), 113.10(11) | 97.29(16),[b] 98.40(17)[b] |
| N–Cu–N | – | 112.0(2) | 163.96(19), 152.3(3), 101.1(3)[c], 106.0(3)[c] |
| Cu–S–Cu | – | – | – |
| Cu–X–Cu | 76.900(14) | 83.759(17), 61.06(2), 111.899(16), 61.34(2), | – |

109.304(19), 83.089(17)

[a]X = Cl, Br, I. [b]X = $ONO_2$. [c]$N_{MeCN}$. [d]Full formula = [Cu(**3**)$_2$]$NO_3$•1.5acetone; solvent molecules removed with Platon SQUEEZE [11].

Table 4. Comparison of Selected patp Bond Distances (Å) and Angles (deg) between **13** [17] and $[Cu_2(NO_3)(\mathbf{13})_2(MeCN)]NO_3$.

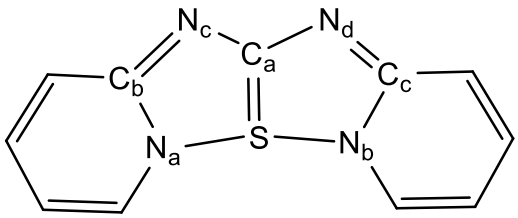


| | **13** | $[Cu_2(NO_3)(\mathbf{13})_2(MeCN)]NO_3$ |
|---|---|---|
| $C_a$–S | 1.782(3) | 1.770(5), 1.756(5) |
| S–$N_a$ | 1.962(2) | 1.942(5), 1.935(4) |
| S–$N_b$ | 1.889(2) | 1.938(5), 1.938(4) |
| $N_a$–$C_b$ | 1.346(4) | 1.355(7), 1.347(7) |
| $C_b$–$N_c$ | 1.353(3) | 1.370(7), 1.367(7) |
| $N_c$–$C_a$ | 1.330(4) | 1.323(7), 1.342(7) |
| $C_a$–$N_d$ | 1.331(3) | 1.343(7), 1.336(7) |
| $N_d$–$C_c$ | 1.349(3) | 1.367(7), 1.381(6) |
| $C_c$–$N_b$ | 1.352(3) | 1.347(7), 1.330(6) |
| $N_a$–S–$N_b$ | 165.50(10) | 165.14(19), 165.07(19) |
| $N_a$–S–$C_a$ | 82.26(12) | 82.6(2), 82.8(2) |
| $C_a$–S–$N_b$ | 83.27(12) | 82.5(2), 82.3(2) |

Contents Entry:

**Copper(I) Complexes of Heterocyclic Thiourea Ligands.**
*Aakarsh Saxena, Emily C. Dugan, Jeffrey Liaw, Matthew D. Dembo and Robert D. Pike**

Synopsis:

Self-assembly reactions of CuX = CuCl, CuBr, CuI, and $CuNO_3$ with heterocyclic thiourea ligands (HetTu) yielded products having CuX:HetTu ratios ranging from 1:1 – 1:5. Twelve X-ray structures revealed a variety of HetTu coordination modes, including S-bridged, X-bridged and/or S/N-chelated monomers 1D polymers and 2D networks. HetTu oxidative cyclization to thiazoles was seen in two cases.

Drawing: